

PHYSICS OF OUR DAYS

Electron theory of metals and geometry

To cite this article: Moisei I Kaganov and I M Lifshits 1979 *Sov. Phys. Usp.* **22** 904

View the [article online](#) for updates and enhancements.

Related content

- [SOME PROBLEMS OF THE ELECTRON THEORY OF METALS III. KINETIC PROPERTIES OF ELECTRONS IN METALS](#)
I M Lifshitz and Moisei I Kaganov
- [SOME PROBLEMS OF THE ELECTRON THEORY OF METALS II. STATISTICAL MECHANICS AND THERMODYNAMICS OF ELECTRONS IN METALS](#)
I M Lifshitz and Moisei I Kaganov
- [Dynamic equations of the theory of elasticity of metals](#)
V M Kontorovich

Recent citations

- [Life on the edge: a beginner's guide to the Fermi surface](#)
S B Dugdale
- [Local geometry of the Fermi surface and its effect on the electronic characteristics of normal metals](#)
Natalya A. Zimbovskaya
- [Local geometry of the Fermi surface and its effect on the electronic characteristics of normal metals](#)
Natalya A Zimbovskaya

Electron theory of metals and geometry

M. I. Kaganov and I. M. Lifshits

Usp. Fiz. Nauk 129, 487-529 (November 1979)

Modern electron theory of metals abounds in geometric terminology and, by using geometric ideas, provides clear descriptions of many complicated phenomena. Some problems in the theory of normal metals that can be interpreted geometrically are examined in this paper in a language accessible to many physicists. Particular attention is devoted to those phenomena and properties that are connected with qualitative (topological) changes in geometric figures such as Fermi surfaces, plane sections though such surfaces, "belts" on the Fermi surface, and so on. Graphical illustrations of these ideas are provided.

PACS numbers: 71.10. + x, 71.25.Pi

The last two to three decades are generally acknowledged as being a period of great progress in the quantum physics of the solid state and, in particular, the quantum theory of metals. There is no doubt about this even if we ignore the development of the microscopic theory of super-conductivity (which is outside the framework of this review).

Considerable experimental evidence has been available for a relatively long time that there are substantial differences between different metals. Thus, it has become clear that the resistance of some metals at low temperatures increases with increasing magnetic field by a considerable factor, whereas that of other metals varies relatively little. It has also been found that the periods of magnetic oscillations in, say, bismuth and gold differ by many orders of magnitude. Such examples could be continued indefinitely. Only twenty years ago, the theory was dealing with a "faceless" metal, whose general properties were described in terms of the degenerate Fermi gas. Most attention was devoted at the time (at any rate, in accounts of the electron theory of metals such as those given in the well-known books by Peierls, Bethe and Sommerfeld, and Wilson) to those topics that the theory was capable of treating, namely, the temperature dependence of resistance, thermal conductivity, specific heat, and so on.

On the other hand, one of the achievements of the *modern* electron theory of metals was the removal of this conflict between theory and experiment. Metals were given their "individuality." It became clear that electrons in some metals differed from those in other metals, and that the "face" of a metal, or its "visiting card", is the Fermi surface, i.e., the equal-energy surface separating occupied states in quasimomentum space from empty states (at absolute zero). Fermi surfaces have been found to be so different and so tortuous that they seem to originate in the imagination of a modern artist instead of being a convenient device for the quantitative description of the properties of conduction electrons.

The development of the electron theory of metals in

its present form, which resulted in the specification of the properties of electrons in different metals, became possible because of the introduction into the theory of metals of geometric pictures and the use of geometric terminology. Contemporary papers on the physics of metals bristle with terms such as "Gaussian curvature", "extremal section", "reference plane", and so on.

The aim of this review is to give a large number of examples demonstrating the usefulness of the geometric interpretation. It has become clear in the course of development of the electron theory of metals that a special role is played by those properties and phenomena which, firstly, are determined by particular groups of electrons lying on certain surfaces and lines, and at certain points and, secondly, are connected with qualitative changes, under external disturbances, in the geometric figures that play an important part in determining the electron properties of metals (surfaces, sections, and "belts"). This will, of course, be considered in some detail below.

1. THE FERMI SURFACE. THE ENERGY SPECTRUM OF METALS

Although there is no rigorous proof of the following proposition, we are, nevertheless, confident that near the ground state, the energy spectrum of any crystal can be described in terms of quasiparticles, where the state of a particular quasiparticle is determined by its quasimomentum p in the periodic p -space whose structure is determined by the geometry of the crystal. All quasiparticles are divided into two groups, bosons and fermions, where the former can, in turn, be divided into many types (phonons, magnons, excitons, and so on), whereas the only fermions are the electrons.

Quasiparticles in the form of bosons form an almost ideal gas in which the interaction between particles decreases with decreasing temperature T simply because there are fewer boson quasiparticles at low temperatures (the number of phonons is proportional to T^3 , the number of magnons in ferromagnets is proportional to

$T^{3/2}$). The temperature dependence of the numbers of bosons, and hence the temperature dependence of many of the physical parameters of crystals, depend on the dispersion relation obeyed by the quasiparticles, i.e., on the relation between the quasiparticle energy ε and its quasimomentum \mathbf{p} :

$$\varepsilon = \varepsilon(\mathbf{p}). \quad (1)$$

This means that, at least in principle, one can use the temperature dependence of experimentally determined parameters of a solid to deduce the Bose branches of its spectrum (or, more precisely, the density of states). Although this method has been justified mathematically,¹ it has been found that methods based on the interaction between penetrating radiation and bosons are the most productive. Since bosons can be created one at a time, and the probability of creating one boson (if it is not forbidden by the selection rules) is greater than the probability of creating more than one boson, inelastic scattering (of neutrons or photons) or resonance absorption¹⁾ (of phonons or photons) can be used to determine the dispersion relations obeyed by the bosons.

The number of conduction electrons in a metal is constant. It follows that a reduction in temperature does not reduce the interaction between electrons, which remains of the same order as the interaction with the lattice ions. The conduction electrons in a metal form a kind of electron liquid, and the development of a systematic theory is possible because this liquid is close to its ground state in practically all cases that are of interest (since $T \ll \varepsilon_F$, where ε_F is the Fermi energy). According to the Landau theory of Fermi liquids, the basic characteristics of the electron subsystem of a metal are the following:

(a) the dependence of the quasiparticle energy on the quasimomentum, $\varepsilon = \varepsilon(\mathbf{p})$, which is given by the variational derivative of the electron energy E with respect to the distribution function $n(\mathbf{p})$:

$$\frac{\delta E}{\delta n(\mathbf{p})} = \varepsilon(\mathbf{p}) \quad (2)$$

(b) the correlation function (Landau function) $f(\mathbf{p}, \mathbf{p}')$, which determines the change in the quasiparticle energy $\varepsilon(\mathbf{p})$ due to a change in the distribution of electrons in \mathbf{p} -space:

$$\frac{\delta \varepsilon(\mathbf{p})}{\delta n(\mathbf{p}')} = \frac{\delta^2 E}{\delta n(\mathbf{p}) \delta n(\mathbf{p}')} = f(\mathbf{p}, \mathbf{p}'). \quad (3)$$

In the ground state (at $T=0$), the electrons occupy all states with energy less than the Fermi energy ε_F . The normalization condition (number of quasiparticles equal to the number of electrons in partially filled bands³⁾) determines the volume occupied by electrons in \mathbf{p} space. The degeneracy of the electron liquid leads to the singling out of Fermi electrons because, when the excitation is weak, the only electrons that are redistributed are those lying near the Fermi surface

$$\varepsilon(\mathbf{p}) = \varepsilon_F. \quad (4)$$

A small change in the electron energy is determined by its velocity

$$d\varepsilon(\mathbf{p}) = \mathbf{v}_F d\mathbf{p},$$

where \mathbf{v}_F is the electron velocity on the Fermi surface. The determination of the electron energy spectrum within the framework of the Landau theory of the Fermi liquid is thus reduced to the determination of the Fermi surface (4) and electron velocity \mathbf{v}_F on this surface. A complete description of conduction electrons must, in addition, include the specification of the Landau function (or, more precisely, matrix) $f(\mathbf{p}, \mathbf{p}')$.

The problem of determining the electron energy spectrum of metals from experimental data (mainly properties in relatively high magnetic fields) was formulated prior to the development of the theory of the Fermi liquid. Naturally, this was done in terms of the "gas" language. It is important to emphasize that most of the methods that could be used (and, in principle, make it possible to determine the different geometrical characteristics of the Fermi surface (see below) have turned out to be unchanged when we "translate" from the "gas" to the "liquid" terminology. This means that:

(a) the characteristics that are determined are indeed those of the surface (4), where $\varepsilon(\mathbf{p})$ is the dispersion relation for the quasiparticle [see (2)] and not for the electron, which does not interact with other electrons

(b) the formulas relating the measured quantities to the characteristics of the dispersion relation for electrons frequently do not contain the Landau function $f(\mathbf{p}, \mathbf{p}')$.

Of course, the Landau function cannot be totally eliminated from the electron theory of metals (i.e., the theory cannot be totally rewritten in the gas language) because $f(\mathbf{p}, \mathbf{p}')$ enters explicitly in the high-frequency, nonlinear, and other characteristics of metals. Determinations of the Landau function belong to a separate, complicated problem and have been much less successful than reconstructions of the Fermi surface.

The determination of the energy spectrum of macroscopic bodies is part of the determination of the characteristics of these bodies. Ideally, the program for achieving a theoretical understanding of the properties of solids would involve, first, the interpretation of the necessary characteristics of the quasiparticles of the given body, followed by the evaluation on this basis of any of its macroscopic characteristics. The scattering cross sections or the mean free paths of the quasiparticles must be known before the transport coefficients can be calculated. If we confine our attention to linear properties of metals, the range of problems for which the gas-kinetic description is sufficient is very large. It includes, firstly, all quasistatic problems [$\omega\tau \ll 1$, where ω is the frequency of the external disturbance and τ is the relaxation time (see Ref. 4, Sec. 2)] and, secondly, problems such as the anomalous skin effect⁵ in which the electron distribution function has a peak in a small region of \mathbf{p} space. Since the Fermi-liquid effects require the addition to the energy of a term con-

¹⁾In quasiparticle terminology, resonance absorption is the transformation of one quasiparticle into another (for example, a photon into an optical phonon).

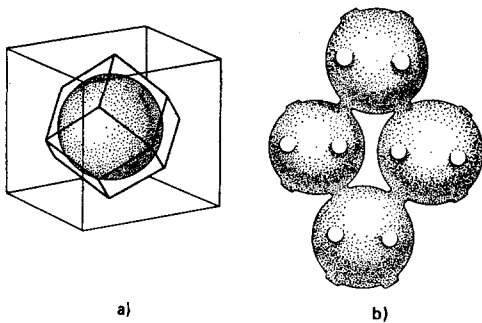


FIG. 1. Closed and open Fermi surfaces: a—closed Fermi surface of an alkali metal; b—open Fermi surface of copper.

taining an integration with respect to the quasimomentum, such effects play a minor role in these problems.

Finally, one should emphasize one other important point which will facilitate the solution of many problems. An electron in a metal is, of course, an extremely quantum-mechanical entity. The band structure of the energy spectrum and concepts such as quasimomentum, quasiparticle, degeneracy, Fermi energy, and so on, arise from the application of the laws of quantum mechanics to electrons. However, the motion of a quasiparticle with quasimomentum \mathbf{p} and energy $\epsilon(\mathbf{p})$ in external fields is, in most cases, quasiclassical. This is so because the external fields are relatively weak in comparison with interatomic fields, and vary over distances that are large in comparison with atomic distances. This, in turn, means that the quasiclassical character of the motion in external fields can be seen, above all, in the fact that the quasimomentum can be regarded as the same as ordinary momentum and $\epsilon(\mathbf{p})$ can be taken to be the Hamiltonian for the "free" quasiparticle, so that a detailed analysis can be made of the motion of the quasiparticles in external fields,⁶ and the results can be used to calculate the parameters of the metal. The Fermi surface—its shape, symmetry elements, and dimensions—provides the same kind of characterization of the solid as its crystal lattice. The periodicity of the \mathbf{p} -space enables us to confine our attention to one cell which, of course, completely determines the Fermi surface. However, it is often more convenient to use the infinite \mathbf{p} -space rather than a single cell. This enables us to distinguish between closed Fermi surfaces, i.e., those that contain periodically repeating cavities (Fig. 1a), and open surfaces, i.e., those running continuously throughout all \mathbf{p} -space (Fig. 1b). Simply-connected surfaces on the Fermi surface can be divided into electron (Fig. 2a) and hole (Fig. 2b) regions, if we separate out the special class of compensated metals with equal numbers of

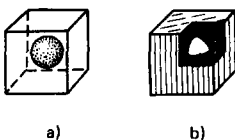


FIG. 2. Electron (a) and hole (b) Fermi surface. States in \mathbf{p} -space, occupied by electrons, are shown black.

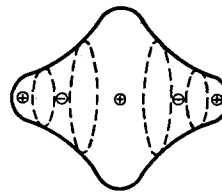


FIG. 3. Elliptic, hyperbolic, and parabolic points on the Fermi surface (the sign of the Gauss curvature K is indicated). Broken lines are lines of parabolic points on which $K=0$.

electrons (n_1) and holes (n_2).²⁾

The local geometry of the Fermi surface (the geometry at a point on the surface) plays an important role in the evaluation of many of the electron characteristics. Apart from the electron velocity $\mathbf{v}(\mathbf{v} = \nabla_{\mathbf{p}} \epsilon)$ is perpendicular to the Fermi surface), it is characterized, as is any surface, by the Gaussian curvature K . All points on the Fermi surface can be divided into

- elliptic
- hyperbolic (or saddle)
- parabolic.³⁾

They are shown in Fig. 3. It will become clear later that parabolic points may be different, depending on the structure of the Fermi surface.

The Fermi surface is the stage on which the "drama of the life of the electron" is played out. And, in the same way in which the life of mountain people is essentially different from people living in the valleys, the properties of electrons in lead, which has an exceedingly complicated Fermi surface (Fig. 4), do not resemble the properties of electrons in sodium, whose Fermi surface is a sphere that is much smoother than a billiard ball. However, on the other hand, both have something in common with the electrons in the degenerate Fermi gas.

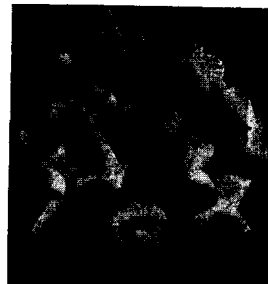


FIG. 4. Part of the Fermi surface of lead (band 3). An example of a "monster" complex open Fermi surface.

²⁾ n_1 is the number of occupied electron states with positive effective mass ($m^* > 0$) and n_2 is the number of empty states with $m^* < 0$ [see (9)].

³⁾ The existence of a parabolic point is a consequence of a change of sign of one of the principal curvatures of the Fermi surface.

2. PLANE SECTIONS THROUGH THE FERMI SURFACE

A. de Haas-van Alphen effect

Shoenberg's celebrated paper⁷ on the oscillatory dependence of the magnetic moment of bismuth on the magnetic field (de Haas-van Alphen effect) had a stimulating effect on reconstructions of the electron energy spectrum of a metal from experimental data. It demonstrated the seemingly unlimited possibilities of quantum magnetic oscillations as sources of information on the parameters of the electron gas in a metal. Shoenberg used expressions resulting from an analysis of the oscillatory properties of the gas of electrons with a quadratic dispersion relation (the Jones model of bismuth⁸) to interpret the experimental data. General formulas relating the dependence of the magnetic moment M on magnetic field H with the parameters of the electron energy spectrum of the metal were not available. Nor was it clear which particular features of the de Haas-van Alphen effect were most important for spectroscopic problems. Nowadays, it is difficult to imagine how much effort had to be expended, for example, to describe the envelope function $M = M(H)$ and how much terminology had to be introduced in order to bring some order into the rapidly accumulating data on the de Haas-van Alphen effect. In the end, Cambridge and Kharkov physicists showed (we are speaking here of the 1950's) that the de Haas-van Alphen effect was a general property of metals.

The phrase "electron with an arbitrary dispersion relation," i.e., nonspecific dependence of energy on momentum, appeared in the theory at about the same time. It turned out that the dispersion relation did not have to be specified in many of the calculations. For example, the magnetic-field dependence of the magnetic moment of electrons with an arbitrary dispersion relation, was used to construct the theory of the de Haas-van Alphen effect.⁹ The development of the physics of metals in the 1950's-1960's was characterized by a definite style of theoretical papers whose structure can be described as follows:

(A) Investigation of the classical motion of an electron with an arbitrary dispersion relation in a magnetic field, using the equations

$$\frac{d\mathbf{p}}{dt} = \frac{e}{c} [\mathbf{v} \times \mathbf{H}], \quad \mathbf{v} = \frac{\partial \epsilon}{\partial \mathbf{p}}. \quad (5)$$

(B) Quasiclassical quantization (whenever necessary) of the classical motion investigated in (A).

(C) Evaluation of the observed parameters, using the results of (A) and (B) and taking into account the degeneracy of the electron gas.

(D) Elucidation and emphasis of spectroscopic possibilities of the phenomenon, i.e., identification of the particular characteristics of the Fermi electron that can be determined from the particular phenomenon under investigation.

The ultimate (although not achievable in practice) aim of papers of this kind was seen by their authors as being a detailed determination of the Fermi surface and of

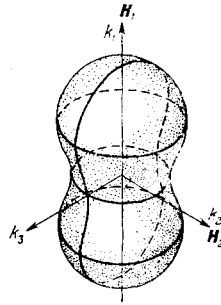


FIG. 5. Plane sections of the Fermi surface with extremal areas.

the velocities of the Fermi electrons. Many of the Fermi surfaces were referred to as "monsters" and the velocities (at right-angles to the Fermi surface) as their "stubble". The ultimate "unshaven monster" was particularly frightful when the surface had internal cavities (with inward "stubble").

Let us now return to Ref. 9:

(1) According to (5), the trajectory of an electron in p -space is the intersection of its equal-energy surface with the plane $p_x = \text{const} (H_x = H_y = 0; H_z = H)$:

$$\epsilon(p_x, p_y, p_z) = \epsilon_0, \quad p_x = p_{z0}. \quad (6)$$

(2) If the trajectory is closed, the motion in the plane perpendicular to the magnetic field is quantized, and the dependence of energy on p_x in the n -th Landau subband is given by the quasiclassical quantization condition^{10,11}

$$S(\epsilon, p_x) = \frac{2\pi e \hbar H}{c} \left(n + \frac{1}{2} \right), \quad n \gg 1, \quad (7)$$

where n are integers and $S(\epsilon, p_x)$ is the area enclosed by the trajectory (6).

(3) The presence of singularities on the boundaries of the subbands (with given n) identifies the extremal (in p_x) sections $S_{\text{ext}}(\epsilon)$, while degeneracy fixes the energy $\epsilon = \epsilon_F$. The Poisson formula then enables us to write down the thermodynamic potential Ω and hence the magnetic moment M in the form of a sum of oscillating terms, each of which is connected with an extremal (in p_x) section of the Fermi surface (Fig. 5), where the period of the oscillations $\Delta(1/H)$ is inversely proportional to the area of the extremal cross section⁴⁾

$$\Delta \frac{1}{H} = \frac{2\pi e \hbar}{c S_{\text{ext}}(\epsilon_F)}, \quad (8)$$

and the function describing the temperature dependence of the amplitude contains the effective mass

$$m^*(\epsilon_F, p_x^{\text{ext}}) = \frac{1}{2\pi} \left. \frac{\partial S(\epsilon, p_x)}{\partial \epsilon} \right|_{\substack{\epsilon = \epsilon_F \\ p_x = p_x^{\text{ext}}}}. \quad (9)$$

(4) By varying the direction of the magnetic field, by measuring the periods and amplitudes, and by compar-

⁴⁾The oscillatory character of Ω and M with period given by (8) is a consequence of the periodic dependence of the density of electron states on $1/H$. This is why practically all the parameters of the metal have an oscillatory dependence on $1/H$ under conditions favorable for the observation of the de Haas-van Alphen effect ($\hbar\omega_c, T \ll \epsilon_F; \omega = eH/m^*c$ is the cyclotron frequency).

ing the experimental results with the above formulas, one can establish both the shape of the Fermi surface and the velocity of Fermi electrons.

The "ideal" program came to a conclusion with the geometric investigation by Lifshits and Pogorelov,¹² who showed that, if a surface has a center of symmetry,^{4a)} there exists an analytical procedure for determining its shape from the periods and the velocities, from, the effective masses [see formulas (17.7) and (17.8) in Ref. 4]. In spite of all the difficulties, this program was actually used to interpret the Fermi surfaces of aluminum and lead.¹³

B. Size effects

The oscillations can be calculated without knowing the motion of the electron with arbitrary dispersion relation in r -space. However, this is necessary in most transport problems and, here, a geometric theorem, which is a consequence of (5), comes to our aid. This states that the projection of the r -trajectory onto a plane perpendicular to the magnetic field can be obtained from the p -trajectory by rotation through $\pi/2$ and by changing the scale: the conversion factor is $c/|e|H$. Motion along the z axis, i.e., along the magnetic field, is described by the function

$$v_z(t) \equiv v_z(p_x(t), p_y(t), p_z = p_{z0}).$$

The quantization condition is particularly apparent, in terms of the r -trajectory; in electron trajectory encloses a magnetic field flux $\Phi = (n + 1/2)\Phi_0$ where $\Phi_0 = 2\pi\hbar c/e$ and n is an integer.

The one-to-one correspondence between the trajectories in p - and r -spaces has given rise to studies of the shape of the Fermi surface based on various size effects.

Size effects are founded on a relatively simple point. The formulation of the problem identifies electron trajectories of a particular size d , which is known (thickness of plate,¹⁴ wavelength of sound wave,¹⁵ and so on). The equation

$$\frac{cD_F}{eH} = d,$$

where D_F a selected diameter of the Fermi surface (for example, an extremal diameter, as in Fig. 6), shows that, when $H = H_d = cD_F/ed$, something should be observed. Theory then predicts *what* will be observed

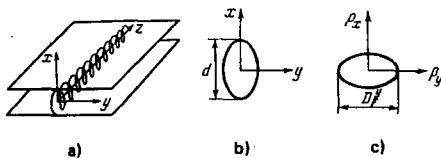


FIG. 6. Nature of size effects based on the correspondence between electron paths in p - and r -spaces: a—orbit in plate of thickness d , b—its projection onto $z = \text{const}$ plane, c—orbit in p -space.

^{4a)}Moreover, the vector p drawn from the center of the surface must not cut the Fermi surface more than once.

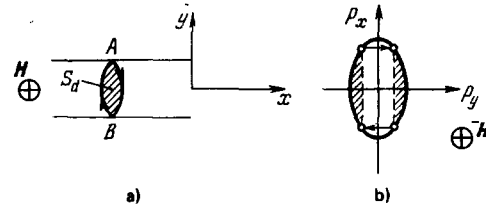


FIG. 7. a—Electron moving in a magnetic field is reflected from the plate surfaces at A and B; b—change in electron velocity on reflection corresponds to hops in p -space (shown by arrows). According to the quantization condition, the magnetic flux through S_d is equal to a half-integral number of flux quanta.

(see Ref. 16). It also establishes the reason for singling out the particular diameter D_F . Measurement of H_d in the size effect is thus a way of determining directly the diameter of the Fermi surface. Anisotropy of the effect (dependence of H_d on the direction of the magnetic field) is a measure of the anisotropy of the electron spectrum, and studies of the anisotropy are a way of probing directly the shape of the Fermi surface.

The size effect and the de Haas-van Alphen oscillations are jointly responsible for particular phenomena that also have a simple geometric interpretation. Figure 7 shows that the electron hops over from one point on the Fermi surface to another as a result of mirror reflection from the surface of the plate. The area S_d (see Fig. 7) appears in the quantization condition (7), which ensures that the period (8) depends on the plate thickness. This phenomenon, predicted as far back as 1953 (see Ref. 17), was found relatively recently in antimony "whiskers."¹⁸

C. Galvanomagnetic phenomena

Galvanomagnetic phenomena (dependence of resistance on magnetic field, Hall effect) are very dependent on the nature of the electron motion in the magnetic field. This is particularly clear in high magnetic fields ($cD_F/eH \ll l$, where l is the electron mean free path) when the electron, between collisions, manages to "feel" the shape of the path on which it is moving. In the opposite limiting case ($cD_F/eH \gg l$), the segment of the path of the electron between collisions is practically a straight line.

The paths of electrons in a magnetic field (6) admit of

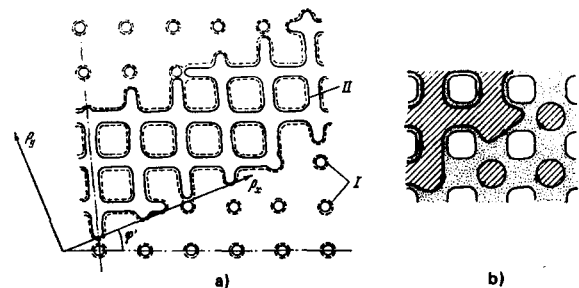


FIG. 8. a—Figure borrowed from Ref. 20, showing the origin of open orbits in metals such as copper, gold, and silver (monster Fermi surface); b—open path separates regions occupied by hole and electron orbits (schematic).

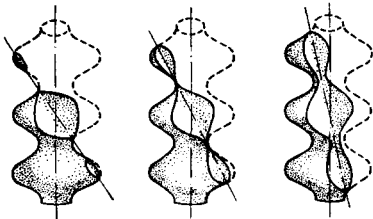


FIG. 9. Self-intersecting trajectory can occur when a Fermi surface in the form of a corrugated cylinder is cut by a plane.

a simple topological classification based on the symmetry properties of the dispersion relation. Two cases are possible: for a given direction of the magnetic field H , the trajectory (6) can either split into closed trajectories or, in the case of an open Fermi surface, go off to infinity in the direction in which the surface is open (Fig. 8). For chosen directions of H and fixed values of p_x , the paths can cross themselves (Fig. 9), or two-dimensional grids of open self-crossing paths may appear (Fig. 10). We shall not, for the present, pause to consider these relatively rare and not well studied cases.

Analyses have shown¹⁹⁻²¹ that galvanomagnetic phenomena, i.e., the dependence of the transverse resistivity on the magnetic field, $\rho_{\perp} = \rho_{\perp}(H)$, and the Hall effect, enable us to "see" the overall shape of the Fermi surface—its topology. It turns out that the asymptotic behavior of the resistivity tensor $\rho_{\alpha\beta}(H)$ in high fields (strictly speaking, as $H \rightarrow \infty$) is very sensitive to the geometry of the Fermi surface.

Geometric characteristics are compared with strong-field behavior in Table I, which can be used as a recipe for determining the topology of the Fermi surface. The entire picture would be more readily interpretable if it were not complicated by the different roles of electrons and holes (Fig. 2). The point is that the quantities $\rho_{\alpha\beta}$ are determined not only by the components of the symmetric part of the conductivity tensor $\sigma_{\alpha\beta}$ but also by its antisymmetric part. The former describe dissipative processes and the latter the Hall effect. In a strong magnetic field

$$\sigma_{xy} = \frac{(n_1 - n_2)ec}{H} + \dots, \quad (10)$$

where $n_{1(2)}$ is the number of electrons (holes) per unit volume [$n_{1(2)} = 2\Delta_{1(2)}/(2\pi\hbar)^3$, where $\Delta_{1(2)}$ is the volume of occupied (empty) states with positive (negative) effective mass]. The dots in (10) indicate omission of higher-order terms in the reciprocal of the magnetic field. It is clear that, when $n_1 = n_2$, the expansion begins with terms proportional to $1/H^2$. This is why $\rho_{\perp} \sim H^2$ for a compensated metal (i.e., when the numbers of elec-

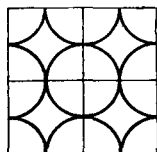


FIG. 10. Two-dimensional net of open self-intersecting trajectories.

TABLE I. Connection between the asymptotic behavior of transverse resistivity and the structure of the energy spectrum.

Closed Fermi surfaces		Open Fermi surfaces
$n_1 \neq n_2$	$n_1 = n_2$	

θ —direction of magnetic field relative to crystallographic axes; for $\theta = \theta_1$, the layer of open trajectories has its maximum thickness; for $\theta = \theta_2$, there are no open trajectories.

trons and holes are equal).

To elucidate the significance of an open Fermi surface, we must consider calculations based on the transport equation. It is sufficient to use a generalization of the Einstein relation

$$\sigma \approx \frac{ne^2\mathcal{D}}{eF}, \quad (11)$$

where σ is the conductivity and \mathcal{D} is the diffusion coefficient, to the case of degenerate statistics, and to use qualitative descriptions taken from kinetic theory to calculate the diffusion coefficient.

When an electron moves in a magnetic field over a closed trajectory, diffusion in the plane perpendicular to the field takes place in jumps by an amount approximately equal to $r_H \approx cD_F/eH$ (Fig. 11) with frequency $\approx 1/\tau$, where τ is the relaxation time. We then have $\mathcal{D} \approx r_H^2/\tau$, and

$$\sigma \approx \frac{\sigma_0}{(\omega_c\tau)^2}, \quad \omega_c = \frac{eH}{m^*c}, \quad (12)$$

where σ_0 is the conductivity at $H=0$.

If the path in p -space along the p_x axis is open, then motion along the y axis in r -space resembles free motion, so that $\mathcal{D}_{yy} \approx v_F^2\tau$, whereas motion along the x axis is practically indistinguishable from a closed orbit, so that $\mathcal{D}_{yy} \approx r_H^2/\tau$. Hence,

$$\sigma_{xx} = \frac{\sigma_0}{(\omega_c\tau)^2}, \quad \sigma_{yy} \approx \sigma_0. \quad (13)$$

The substantial difference between the asymptotic behavior of $\sigma_{xx}(H)$ and $\sigma_{yy}(H)$ is responsible for the anist-

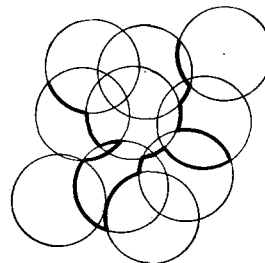


FIG. 11. Diffusion of an electron in the plane perpendicular to the magnetic field. Thick line shows the random diffusion path.

copy of the galvanomagnetic properties of metals with an open Fermi surface (see Refs. 19–21 and Ref. 4, Secs. 27 and 28).

An understanding (through geometric analysis) of the motion of electrons in a magnetic field frequently leads to predictions of very unusual phenomena. These undoubtedly include the static skin effect²² in which surface conductivity in a strong magnetic field turns out to be appreciably greater than the bulk conductivity.

Suppose that the magnetic field is parallel to the surface of the specimen. Specular reflection of electrons from the surface ensures that their motion within the surface layer ($\approx r_H$) in the direction perpendicular to the magnetic field resembles motion over an open path (Fig. 12a), so that one of the components of the surface conductivity (σ_{yy}) is greater by a factor $(\omega_c \tau)^2$ than the bulk conductivity (to be specific, we assume that the Fermi surface is closed). Diffuse scattering does not remove this effect. As a result of collisions, whose frequency is $\approx \omega_c$, the mean transport of electrons directly on the boundary of the specimen is approximately equal to r_H , and $\sigma_{yy}(z=d)$ turns out to be approximately equal to $\sigma_0/\omega_c \tau$. At a distance of approximately r_H from the boundary, the situation is substantially modified because the magnetic field "makes" all the electrons that have been reflected from the boundary travel to one side, so that σ_{yy} rises to σ_0 (Fig. 12b). It is clear, even from the foregoing, that the static skin effect is not such a simple phenomenon as would appear from a "handwaving" account. The derivation of the formulas must be based on the solution of the transport equation in the inhomogeneous case and a careful analysis of the particular situation, i.e., the relationship between the plate thickness d , the mean free path l , and the electron-orbit radius r_H . Moreover, the spectrum of the electrons is important: is the Fermi surface closed or open is the metal compensated or not. Not all the predictions of the theory²³ relating to the static skin effect have been experimentally confirmed, but there is no doubt that, in a strong magnetic field, the conductivity near the sample surface may well be higher than within the body of the metal.

The qualitative change in the motion of a conduction electron in a magnetic field, due to the inhomogeneity in the Lorentz force acting on the electron, can readily be understood by considering the interaction of an electron with a domain wall²⁴ (180-degree boundary between domains, Fig. 13). The conductivity along the domain wall should be higher by a factor $(\omega_c \tau)^2$ than in the per-

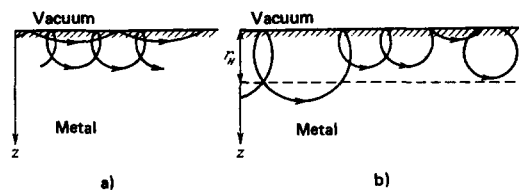


FIG. 12. An open orbit can arise as a result of reflection of the electron from the boundary of the metal specimen: a—specular reflection; b—diffuse reflection. In both cases, the electrons are driven by the magnetic field in one direction and the holes in the other.

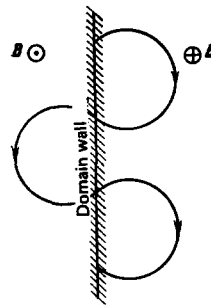


FIG. 13. Open orbits can arise near the domain walls because the Lorentz force changes sign between domains.

pendicular direction.

This cursory examination of the theory of galvanomagnetic phenomena must, in our view, be concluded with a work of caution: the theory^{19,20} claims to derive the asymptotic behavior of $\rho_{ik}(\mathbf{H})$ by analyzing the classical motion of electrons with an arbitrary dispersion relation in a sufficiently strong magnetic field, i.e., when the collision frequency $1/\tau$ is much less than the frequency ω_c of the Larmor precession ($\omega_c \tau \gg 1$ or $cD_F/eH \ll l$, see above).

Quantization of the motion of the electron in the plane perpendicular to the magnetic field makes the classical approach definitely inexact. Quantization leads to oscillations in ρ_{ik} as a function of the reciprocal magnetic field (this is the Shubnikov-de Haas effect²⁵). The Shubnikov-de Haas and de Haas-van Alphen²⁶ effects are of the same kind in particular both have the same periods and are both observed when the motion of the electrons in the magnetic field is quasiclassical ($\hbar \omega_c \ll \epsilon_F$). As a rule, the oscillating quantum part of the resistivity tensor ρ_{ik}^{osc} is appreciably less than the monotonic classical part of $\rho_{ik}(\mathbf{H})$: the oscillations are superposed on the monotonic classical function $\rho_{ik} = \rho_{ik}^{mon}(\mathbf{H})$ in the form of a "ripple". Essentially, this is what enables us to use the classical theory.

The quasiclassical condition ($\hbar \omega_c \ll \epsilon_F$) introduces a further simplification: the collision operator \hat{W} in the Boltzmann transport equation, used to evaluate the galvanomagnetic characteristics,^{19,20} is independent of the magnetic field in zeroth order in $\hbar \omega_c/\epsilon_F$. This is a consequence of the fact that the electron collision length in a crystal containing impurities, which play a dominant role at low temperatures, is of the order of the interatomic distance a , and the condition $a \ll r_H \approx cD_F/eH$ reduces to $\hbar \omega_c \ll \epsilon_F$. The almost total absence of a dependence of \hat{W} on H for scattering by phonons is due to the relatively weak condition $\hbar \omega_c/T \ll v_F/s$, where s is the velocity of sound which, in turn, means that the wavelength λ of a phonon of energy $\hbar s/\lambda \approx T$ is small in comparison with r_H .⁵⁾ The fact that \hat{W} is independent of H

⁵⁾ This condition presents no great problems. Indeed, comparison with the necessary condition $\omega_c \tau \gg 1$ leads to a very weak condition on the mean free path, T (deg) l (cm) $\gg 10^{-6}$. The condition that ρ_{ik}^{osc} be small in comparison with ρ_{ik}^{mon} also contains the temperature: $\hbar \omega_c \ll \sqrt{T \epsilon_F}$. At very low temperatures, it may fail, but, as shown above, not too drastically: l^2 (cm) T (deg) $\gg 10^{-11}$.

essentially enables us to establish the asymptotic behavior of $\rho_{ik}(H)$ on the basis of an analysis of classical electron dynamics.

This relatively simple theory does not fully cover the entire situation. For example, it cannot be used for intermediate fields. Arbitrary fields require numerical calculations, previously quite inaccessible but now gradually replacing analytic methods (authors view this with sadness). There are, however, situations where an analytic treatment is possible in intermediate fields. This means that the various characteristics of a metal include an additional small parameter (or parameters). The simplest case is that where the difference $\Delta n = n_1 - n_2$ is small. For such metals (for example, bismuth containing impurities), the resistivity saturates only when $\omega_c \tau \gg n/\Delta n \gg 1$, whereas, for $n/\Delta n \gg \omega_c \tau \gg 1$, it is a quadratic function of the field, i.e., the metal behaves as if it were compensated.^{27, 28} A similar phenomenon should also occur when the Fermi surface contains a narrow layer of open paths.²⁹

These two parameters are essentially simple. The magnetic field does not "interfere" in either the spectrum of the electrons or their collisions. High fields are necessary to isolate electrons responsible for the asymptotic behavior because the number of such electrons is small. On the other hand, the magnetic field can not only single them out but can also produce them. This will be discussed in the section on magnetic break-through.

One further point: detailed description of collision processes can be used to establish "intermediate" asymptotic behavior, which is undoubtedly of considerable interest. For example, consider the following crude treatment which merely throws some light on the essence of the situation (a more detailed account will be given in the next Section). Suppose there are two groups of electrons with very different mean free times $\tau_1 \gg \tau_2$ and roughly equal masses m_1 and m_2 . In intermediate fields,

$$\frac{m_1 c}{\epsilon \tau_1} \ll H \ll \frac{m_2 c}{\epsilon \tau_2}$$

the second group "feels" the magnetic field as strong, whereas the first "feels" it as weak, and this is, of course, reflected in the dependence of ρ_{ik} on H .

3. ELECTRONS "HOP" OVER THE FERMİ SURFACE

In its stationary state, the electron has a definite quasimomentum \mathbf{p} and rests at its "own" particular point in \mathbf{p} -space. Regular external fields force the electron into phase paths that are particularly simple if the motive force is a constant and uniform Lorentz force (5). As already noted, an electron with energy equal to the Fermi energy then moves over the Fermi surface. However, displacement of electrons in \mathbf{p} -space is not restricted to motion under the influence of regular fields. Scattering plays an important role in the life of electrons, including scattering by impurities, phonons, and each other. In the case of collisions with impurities, dislocations, and other static defects of the crystal, a Fermi electron hops from one point on the

Fermi surface to another because energy is conserved in such collisions.

The scattering of particles with a complicated dispersion relation is characterized by certain specific features.³⁰ They will be discussed below. If the Fermi surface has no dents, each quasimomentum \mathbf{p} corresponds to a particular direction of motion of the electron $\nu = \mathbf{v}/v$ (the quasimomentum is described as the point at which the plane perpendicular to ν is tangent to the Fermi surface; Fig. 14). If the Fermi surface has a more complicated shape, there are directions in which the direction of motion does not uniquely define the quasimomentum \mathbf{p} (Fig. 14). This is responsible for the difference between the scattering of particles with a complicated dispersion relation and the scattering in free space with $\epsilon = \mathbf{p}^2/2m$. Flattened areas on the Fermi surface play a particular role. If the direction of scattering is parallel to the normal at a parabolic point $\nu = \nu_c$ (Fig. 14), there are two equal momenta of the scattered particles, and the wave function for the scattered particle decays more slowly for $\nu = \nu_c$ than for $\nu \neq \nu_c$. This phenomenon has not been extensively studied, but it seems to us that it may play an important role in studies of indirect interactions through conduction electrons of impurity atoms, localized spins, and so on. The scattering of quasiparticles with an arbitrary dispersion relation has been investigated in Ref. 30 (see also Ref. 31).

In the case of collisions between electrons and phonons or other bosons (for example, magnons in ferromagnetic or antiferromagnets), the following points are important: the energy of the quasiparticles (bosons) is, as a rule, small in comparison with the Fermi energy, and their quasimomentum may reach values of the order of the size of a cell in \mathbf{p} -space. One-phonon (one-boson) processes are the most probable: an electron will create or absorb a phonon as a result of a "collision." It is clear that this is an almost-elastic process and, as in the case of elastic collisions, the electron "hops" from one point on the Fermi surface to another.

At low temperatures $T \ll \theta$ (θ is the Debye temperature; this region is particularly interesting from the point of view of the geometric properties of the electron energy spectrum), the number of phonons (or other bosons) with high quasimomenta is exponentially small, and collisions with bosons, whose quasimomentum is much smaller than the average linear dimensions of the

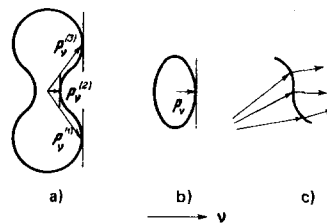


FIG. 14. a—Electrons moving in a given direction ν usually have different quasimomenta \mathbf{p}_v ; b—one quasimomentum corresponds to one direction of motion only in the case of a convex Fermi surface; c—the direction parallel to the normal to the Fermi surface at a parabolic point is limiting direction: two values of the quasimomentum become equal at this point.

Fermi surface, play the dominant role. Motion over the Fermi surface as a result of such collisions can be regarded as a diffusion process. In particular, the diffusion approach can be adopted to provide a "hand-waving" interpretation of the nature of the Bloch temperature dependence of the transport mean free time τ_{tr} of electrons for $T \ll \theta$. The time τ_{tr} is essentially the time taken by an electron to diffuse over a distance approximately equal to D_F , i.e., $\tau_{tr} \approx D_F^2/\mathcal{D}_p$, where \mathcal{D}_p is the coefficient of diffusion over the Fermi surface. However, $\mathcal{D}_p \approx (\Delta p)^2/(1/\tau_{eph})$, where $\sqrt{(\Delta p)^2}$ is the average change in the momentum of the electron as a result of collisions with phonons, i.e., the size of the "hop" over the Fermi surface, and $1/\tau_{eph}$ is the frequency of collisions with phonons, which is proportional to the number of phonons which, in turn, is proportional to T^3 for $T \ll \theta$. Since the average phonon momentum is approximately $D_F(T/\theta)$, it follows that \mathcal{D}_p and $1/\tau_{tr}$ are proportional to T^5 (this is Bloch's law).

The situation changes when electrons in a small part of p -space, for example, electrons in the "neck" in a strong magnetic field (see p. 495 and Fig. 15) are responsible for conductivity. If the linear dimensions of this region are such that a single hop will suffice to take the electron away from the region (the probability that it will reenter the small region of p -space is, of course, slight), then $\tau_{tr}^{-1} \sim T^3$. The frequency of collisions involving electrons whose orbits are closed and which ensure that the conductivity associated with them is inversely proportional to H^2 is, again, described by Bloch's law (see Ref. 29).

It is important to emphasize that collisions in which the change in electron momentum is small (small-angle scattering) often have considerable probability. Their role is frequently reduced because the collisions are ineffective by virtue of the fact that $\sqrt{(\Delta p)^2} \ll D_F$. The example given shows that ineffective collisions can be avoided, which leads to a reduction in τ_{tr} .

Quasimomentum is not conserved in collisions because electrons with quasimomenta that differ by a multiple of the period in p -space are equivalent. Collisions in which the initial quasiparticle momentum differs from the final momentum by the period of p -space are referred to as umklapp collisions or U -processes.³² The stationary state in an ideal (defect-free and infinite) conductor through which a current is flowing could not be established in the absence of U -processes.

It is much more convenient to use the periodic p -space than a single cell in this space, especially in the case of dynamic problems requiring an analysis of the motion of electrons in p -space. It is, however, impor-

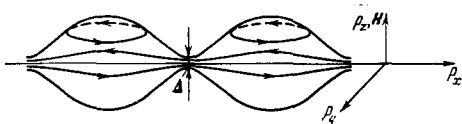


FIG. 15. Electrons whose paths pass through the narrow neck of thickness Δ connecting the "almost closed" cavities of the Fermi surface are responsible for the y conductivity in a strong magnetic field.

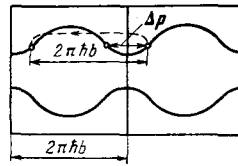


FIG. 16. A hop process (shown by the broken arrow) can occur with an arbitrarily small change in the electron quasimomentum.

tant to recall that all nonequivalent states are contained in a single cell of the p -space, which must be chosen in a particular way. If a collision takes an electron out of the chosen cell, it must be "flipped over", i.e., non-conservation of quasimomentum must be taken into account. The choice of the particular cell in p -space is arbitrary but, in the case of metals, it is convenient to choose the p -space cell in the light of the shape and position of the Fermi surface. For example, in the case of a closed Fermi surface, it is convenient to take the cell so that it contains the entire Fermi surface. The first Brillouin zone is frequently used, but it is not always convenient, for example, in the case of bismuth in which three electron ellipsoids intersect the boundary of the first Brillouin zone. Analysis of possible U -processes is essentially a geometric problem that must be solved directly for each metal. Since the linear dimensions of the Fermi surface are relatively large, U -processes in electron-electron collisions occur with relatively high probability, whereas, in metals with open Fermi surfaces, they can occur with an infinitesimal change in the electron momentum (Fig. 16).

An interesting situation occurs in strong (but not limiting) magnetic fields when the Fermi surface comes close to its analog in a neighboring cell of p -space. Figure 17a illustrates this situation. If the separation between the points of closest approach is much less than the size of the unit cell of the reciprocal lattice, small-angle scattering (by phonons or dislocations) will ensure that U -processes will have considerable probability.³³ These points of closest approach are called hot spots of the Fermi surface. The role of the magnetic field reduces to complete or partial replacement by motion over a diffusive trajectory from one hot spot to another (Fig. 17b). This, of course, emphasizes the

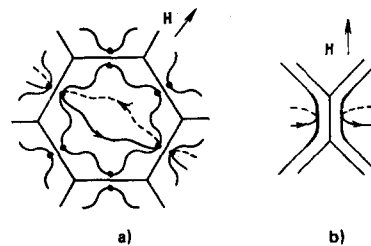


FIG. 17. a—Hot spots on the Fermi surface (motion in a magnetic field accelerates the transfer from one hot spot to another); b—scattering with umklapp may lead to the appearance of an open orbit if the flip-over probability is high enough because of the approach of relatively large segments of Fermi surface: the probability of hopping across to the neighboring cell is greater than the probability of traversing a hot region (shown in figure).

role of umklapp processes. This example demonstrates the fact that the magnetic field "interferes" with collision processes, although the collision itself (its probability) is independent of H . This "interference" of the magnetic field in scattering processes is particularly curious when, owing to the flip-over processes in regions where the Fermi surface approaches its analog in a neighboring cell, the motion of the electron takes place effectively over an open path³⁵ (Fig. 17b). When the magnetic field is strong enough, an open path cannot be formed since the electron traverses the Fermi surface near a hot spot so rapidly that it does not succeed in hopping over onto the neighboring surface.⁶⁾

The last example takes us outside the framework of the internal geometry of the Fermi surface. In the phenomena and properties described so far, the relative disposition of separate parts of the Fermi surface in p -space is quite unimportant. The increased interest in the relative disposition of such cavities, has arisen relatively recently in connection with studies of magnetic breakthrough (see below), size effects due to intervalley scattering,³⁶ and other effects that have so far been studied very little.

4. ELECTRONS WITH AN ARBITRARY DISPERSION RELATION AND THE HARRISON MODEL

Work on the synthesis of Fermi-surface profiles from experimental data has been accompanied, and sometimes even preceded, by calculations of the band spectrum of conduction electrons on the basis of various models of a metal. It seems to us that the Harrison model,³⁷ in which complicated Fermi surfaces can be obtained by cutting through a periodically repeating sphere and combining the spherical segments in a different order, has played an important role in the popularization of computational methods.

If the periodic potential energy $V(r)$, in which the electrons move, is small in comparison with the kinetic energy of the electrons, it can be taken into account in accordance with perturbation theory (this is the Brillouin approximation of nearby free electrons).³⁸ The Harrison scheme for constructing the Fermi surface is as follows:

(1) Plane waves (zero-order approximation) are used to construct the electron wave function Ψ_p , satisfying the Bloch condition

$$\Psi_p(\mathbf{r} + \mathbf{a}) = e^{i\mathbf{p}\mathbf{a}/\hbar} \Psi_p(\mathbf{r}), \quad (14)$$

where \mathbf{a} is the period of the crystal lattice. This step is equivalent to the transformation of momentum into the quasimomentum (Ψ_p is automatically a periodic function of \mathbf{p} : $\Psi_p + 2\pi\hbar\mathbf{b} = \Psi_p$, where \mathbf{b} is a reciprocal lattice vec-

tor).

(2) Spheres having the radius of the Fermi sphere for free electrons $p_F = (3\pi^2 n_v)^{1/3} \hbar$ (n_v is the number of valence electrons per unit volume) are drawn at all points equivalent to $\mathbf{p} = 0$ in the quasimomentum space for the given crystal. If these spheres do not intersect, i.e., each sphere lies inside its own cell, the construction is complete, i.e., the Fermi surface is a sphere. If, on the other hand, the spheres intersect, then

(3) degeneracy must be removed by introducing a correction to the energy which takes $V(\mathbf{r})$ into account in the necessary order or perturbation theory. This local and relatively small change in the energy of the electron produces a radical change in the shape of the Fermi surface.

(4) The concluding stage is the redistribution of electrons from the original sphere over the new pieces of the Fermi surface (Fig. 18).

It is clear from the foregoing that the Harrison construction is a purely geometric problem, more crystallographic than physical.

It is important to note that the Harrison model has always presented difficulties to those who are used to thinking in terms of an arbitrary dispersion relation. The model has been distinguished more by its successes than by its justification³⁹: it gives Fermi surfaces that are similar to those obtained from comparison between experimental data and theory without using any assumptions about the form of $\epsilon(\mathbf{p})$.

The development of several effective methods for numerical evaluation of the electron energy spectrum (the pseudopotential method, OPW, APW, KKR, and so on) has modified our approach to the solution of spectroscopic problems. A particular model and a method of calculating the electron energy spectrum are used to determine the main outline or the possible variants of the Fermi surface and to elucidate the possible limits on changes in the Fermi surface. Experimental data are used simply to improve the model parameters. This gives rise to the ideal scheme:

Model - comparison with experiment - improved model and "global" calculation ...

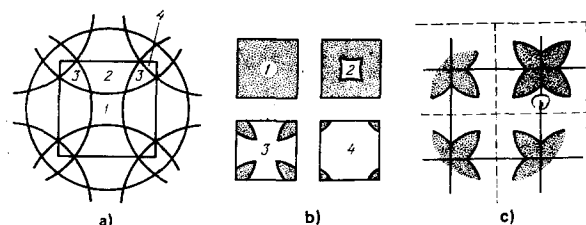


FIG. 18. The Harrison construction in the two-dimensional case: a—original circles (zero-order approximation); b—distribution of electrons over the zones (Fermi surface cavities) as a function of the number of circles covering the p -space region: the number of covers determines the number of the zone (filled states are shown shaded); c—Fermi surface in third zone, combined into a single closed surface (with this zone, it is convenient to use the cells shown by the broken lines).

⁶⁾A more detailed account of the temperature-field dependence of the transport coefficients of pure metals, as determined by the diffusion of electrons over the Fermi surface and hops between hot spots, can be found in the paper by Gurki and Kopeliovich.³⁵ This appears to be the first paper in which the geometry of the Fermi surface (its structure) is taken into account in detail in a discussion of the qualitative properties of the temperature dependence of transport coefficients.

The Fermi surfaces of most simple metals and many intermetallic compounds are now known as a result of the application of this scheme.

All modern models used to construct the electron energy spectrum are essentially developments of the method of nearly free electrons.³⁸ The problem then naturally arises as to what is a conduction electron. Is it an almost free electron whose motion is slightly perturbed by the periodic field of the lattice and by external fields, or is it an electron with a complicated dispersion relation moving under the influence of the external fields? Such questions are often encountered, both explicitly and implicitly. The answer is not a matter of taste but is determined firstly by the formulation of the problem and secondly by the ratio of the lattice field to the external field. Of course, the dispersion relation cannot be determined without some more or less acceptable model. This cannot be avoided, so that if we try to evaluate some particular parameter of a metal—its response to an external field—we have to decide whether we start with a gas of free electrons, which has well-known responses to an external field, or whether we “doctor” the result by taking the lattice field into account. Conversely, we can start with a gas or Fermi liquid of electrons with a complicated dispersion relation, and investigate the motion of particles with a complicated dispersion relation in an external field. The answer is, in fact, decided by comparing the characteristic energy ϵ_{char} of electrons with the energy that is a measure of the interaction between the electron and the external field (we shall denote it by $\Delta\epsilon$). If we are dealing with a constant magnetic field, then $\Delta\epsilon = \hbar\omega_c$ is the separation between the Landau magnetic levels, whereas, if we are dealing with the electric field, then $\Delta\epsilon = eEl$ is the energy acquired by an electron in one mean free path l . Finally, if we are dealing with a high-frequency field, we have $\Delta\epsilon = \hbar\omega$, where ω is the field frequency. If

$$\epsilon_{\text{char}} \gg \Delta\epsilon, \quad (15)$$

we must, of course, consider the reaction of electrons with an arbitrary dispersion relation.

It is important to note that the triumphant progress of the Harrison model and of model calculations generally should lead us to a degree of caution in estimating ϵ_{char} . Some decades ago, it was always assumed in numerical estimates that $\epsilon_{\text{char}} \approx \epsilon_F$ and that the scale of the Fermi energy ϵ_F was determined by the electron density $n = z/a^3$, i.e., $\epsilon_F \approx \hbar^2 z^{2/3} / a^2 m \approx 10^{-12}$ erg $\approx 10^4 - 40^5$ °K, where z is the number of valence electrons per atom and a is the lattice parameter. In other words, it seemed that, so long as the external fields were weak in comparison with atomic fields, there was no problem. It was generally believed that the energy structure of a metal was reasonably permanent and not subject to external modification. The only exception was the fifth group in the periodic table (Bi, Sb, P), but these were virtually semiconductors, i.e., semimetals. It has been gradually recognized, however, that the energy structure of a metal is a relatively delicate entity (model calculations and experimental studies, especially of oscillatory effects, played an important role in

this process). This structure is relatively readily affected by external changes such as pressure, the addition of electrons through the introduction of impurities, and so on. A small change in the model parameters, or a shift in the Fermi energy, can produce an appreciable change in the Fermi surface. Even the appearance of a periodic average magnetization accompanying the transition from the paramagnetic to helicoidal state may lead to a local but sensitive change in the shape of the Fermi surface.⁴⁰ A change in the structure of the electron spectrum is accompanied by a change in the connectivity of the Fermi surface and is described (at $T = 0$) as a peculiar phase transition which in the Ehrenfest nomenclature⁴¹ should be treated as a phase transition of order $2\frac{1}{2}$ (see below).

The recognition of the complexity of the structure of the electron spectrum has led to a considerable modification of estimates of the characteristic energy ϵ_{char} . This energy must be interpreted as $|\epsilon_F - \epsilon_k|$, where ϵ_k is the energy at which there is a change in the topology of the equal-energy surfaces.⁴² The fact that ϵ_{char} is small in comparison with ϵ_F indicates that singular points in p -space are close to the Fermi surface.

More precise formulation of the inequality given by (15) may have very substantial consequences. We shall consider them later (in Sec. 11). For the moment, we return to the concept of an electron with an “arbitrary dispersion relation.” Model calculations have removed its mystical halo. It turns out that the great variety of Fermi surfaces is not as difficult to understand as it seemed twenty years ago. For example, the existence of small groups of conduction electrons in most metals, which was discovered through the study of oscillation effects and which was for long a puzzle, has now been simply explained by the fact that, in polyvalent metals, the initial Fermi spheres used in the Harrison model are found to cross repeatedly. This explanation is supported by the fact that metals in the first group of the periodic table have simple Fermi surfaces.

However, we must emphasize that the description of many of the electronic properties of a metal (thermal, magnetic, galvanic, thermoelectric, radiofrequency, optical, and so on) must start with the idea of the conduction electron as a Fermi particle with a complicated dispersion relation: even when ϵ_{char} is more precisely defined, the inequality given by (15) is easily satisfied in the great majority of cases.

Thus, the elementary charge carrier in a metal is an electron with a complicated dispersion relation, and its state is determined by specifying the quasimomentum p . The fact that this p is a *quasimomentum*, and not simply the momentum, is used in calculating the probability of any particular event, and one must not forget umklapp processes. In all other cases, it is “demoted” to momentum, and the energy $\epsilon(p)$ is interpreted as the kinetic energy of the “free” electron.

5. “BELT” ON THE FERMİ SURFACE

The degeneracy of the electron gas in a metal ($T \ll \epsilon_F$) ensures that only Fermi electrons participate in

the electrical conductivity of a metal and all the accompanying phenomena. Electrons in the Fermi "cellar" drop out of the picture, and simply maintain the number of electrons with $\varepsilon = \varepsilon_F$. This is why the Fermi surface is so important. The cross-sectional area S of the Fermi surface and even the volume $\Delta_{1(2)}$ of the disconnected parts of the Fermi surface are encountered in the formulas given above [the latter in Eq. (10)]. The appearance of geometric figures connected with the internal structure of the Fermi surface has a formal mathematical origin: the contour integral $\oint (dp_{\parallel}/v_{\parallel})$, evaluated over an orbit on the Fermi surface, which determines the period of revolution of the electron, is numerically equal to $[\partial S(\varepsilon, p_{\parallel})/\partial \varepsilon]_{\varepsilon=\varepsilon_F}$, where dp_{\parallel} is the displacement along the path (6) and $v_{\parallel} = \sqrt{v_x^2 + v_y^2}$.

The "discrimination" among electrons is not restricted to the exclusion of electrons in the Fermi "cellar." Since $l \gg r_H$, electrons with closed paths contribute practically nothing to the conductivity of a metal in a strong magnetic field if the Fermi surface contains a layer of open paths. The de Haas-van Alphen and other effects are due to electrons confined to the path whose area is extremal in p_x .

It is particularly striking that most of the conduction electrons contribute very little to the high-frequency properties of metals.

A. Attenuation of ultrasonic waves by electrons

Electrons whose velocity \mathbf{v} satisfies the Cerenkov condition (see Ref. 43)

$$\mathbf{k} \cdot \mathbf{v} = \omega, \quad (16)$$

are responsible for the collisionless interaction between a metal and sound waves (\mathbf{k} and ω are respectively, the wave vector and frequency of the wave). Since the electron fluid is degenerate, absorption involves the participation only of electrons with energies equal to the Fermi energy

$$\varepsilon(\mathbf{p}) = \varepsilon_F. \quad (17)$$

Equations (16) and (17) together define a line on the Fermi surface. It is customary to refer to it as a "belt." Since $\omega/k = s \approx 10^5$ cm/sec $\ll v_F \approx 10^8$ cm/sec, we can frequently assume that $s=0$, i.e., neglect the propagation of the sound wave. This means that the condition for collisionless interaction selects electrons moving at right-angles to the wave vector \mathbf{k} ($\mathbf{v}_{\perp} \mathbf{k}$). The other electrons turn out to be ineffective (the term "ineffective" as applied to electrons was introduced by Pippard⁴⁴).

The "belt" can be satisfactorily represented as the boundary between light and shadow if we "translate" the Fermi surface into ordinary space and direct a parallel beam of light along the wave vector \mathbf{k} (Fig. 19). For a quadratic dispersion relation $\varepsilon(\mathbf{p}) = (1/2)m^{-1}_{ik} p_i p_k$, $v_i = (m^{-1})_{ik} p_k$, where $(m^{-1})_{ik}$ is the reciprocal mass tensor and (16) is the equation of a plane, the "belt" is an ellipse whose axes and orientation depend on the velocity of sound and the direction $\mathbf{n} = \mathbf{k}/k$ of this velocity. If we suppose that $s=0$, the plane de-

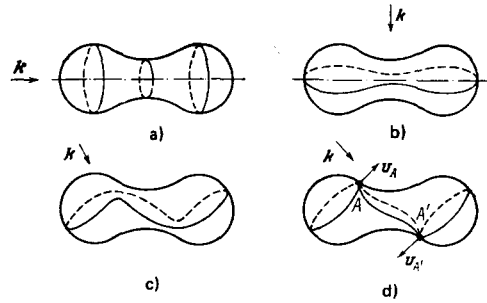


FIG. 19. Belts on the Fermi surface can be simulated by the boundary between light and shadow: the direction of the incident light is that of the wave vector \mathbf{k} of the sound waves (the number of belts and their structure depend on the shape of the Fermi surface and direction of \mathbf{k}): a—vector \mathbf{k} lying along the axis of the dumbbell (three belts); b—vector \mathbf{k} perpendicular to the dumbbell axis (one belt); c—the belt is not, in general, a plane curve; d—the belt can intersect itself: $\mathbf{k} = \mathbf{k}_c$, $\mathbf{k}_c \perp \mathbf{v}_A$, $\mathbf{v}_{A'}$, the points A and A' lie on the locus of parabolic points.

fined by (16) passes through the center of the ellipsoid (the Fermi surface is then a sphere and the belt corresponding to $s=0$ coincides with a great circle). Even a slight complication in the shape of the Fermi surface leads to a very considerable complication in the shape and structure of the belt. Figure 19 shows belts on a surface in the form of a dumbbell for different directions of the wave vector \mathbf{k} .

The expression for the coefficient, for absorption of sound by electrons in the metal when $kl \gg 1$, is (see Refs. 45, 46)

$$\Gamma_e = \frac{2\omega}{(2\pi\hbar)^3 \rho s} \oint_{(F)} |\Lambda|^2 \frac{dS}{v^3} \delta(\mathbf{n} \cdot \mathbf{v} - \frac{s}{v}), \quad \mathbf{v} = \frac{\mathbf{v}}{v}, \quad (18)$$

where ρ is the density of the metal, Λ is a component of the deformation potential modified by screening and determined by the polarization of the sound,⁴⁶ and the δ -function is the limit of the solution of the transport equation when $kl \gg 1$. It is clear that the condition for collisionless absorption, namely, $kl \gg 1$, discriminates against all electrons, other than those in the "belt", which move in the phase plane of the sound wave.

B. Anomalous skin effect

The concept of the "belt" first appeared in the physics of metals in the theory of the anomalous skin effect⁵ describing the reflection of an electromagnetic wave by a metal when the skin-layer depth δ was less or even very much less than the electron mean free path l . When $\delta \ll l$, most of the electrons spend only a very small fraction of their mean free time within the skin layer (under the influence of the electric field of the wave). Electrons moving parallel to the surface of the metal are the only exception to this^{44, 47} (Fig. 20). It is precisely these electrons that participate in the reflection of the electromagnetic wave. This is expressed mathematically by the fact that the surface impedance of the metal is given by a formula in which [as in (18)] the integration over the Fermi surface reduces to integration over the belt defined by (16) and (17).

By displacing the belt over the Fermi surface and measuring the surface impedance of the metal, we can

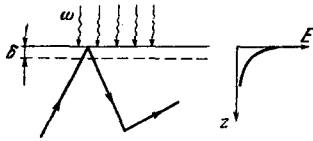


FIG. 20. In the anomalous skin effect ($l \gg \delta$), electrons moving along the boundary of the metal ($v_x = 0$) play the dominant role because they interact with the electromagnetic wave throughout their mean free time.

investigate the structure of the Fermi surface and, as is clear from the formula for the impedance, we can directly determine the Gaussian curvature of the Fermi surface averaged over the belt.^{44, 47} It is difficult to displace only the belt. The electromagnetic wave always propagates at right angles to the surface because of the large optical density of the metal. All this means that the only remaining possibility is the investigation of the impedance of different faces of a single crystal. This was, in fact, done by Pippard,⁴⁸ who used single crystals of copper.

The spectroscopic possibilities of studies of electromagnetic properties of metals are governed by the fact that the charge of a conduction electron is equal to the charge of a free electron (the formula for the impedance involves only the geometric characteristics of the Fermi surface). The situation is worse in the case of ultrasonic waves. As we have seen, the coupling between these waves and electrons is described by the deformation potential,^{49, 50} and the determination of the components of this potential is a problem in itself. It is, therefore, tempting to try to determine the components of the deformation potential (averaged over the belt) for those metals for which the dispersion relation is known, and then use the measured electron part of the sound absorption coefficient Γ_e [Eq. (18)]. For reasons which we cannot understand, this method of determining the deformation potential averaged over the belt has not been very popular (see Ref. 51).

C. Cyclotron resonance

Thus, both the wave and the skin effect isolate the belt electrons. A magnetic field forces the electrons to move over the Fermi surface on paths described by (6) which, in general, cut the belt at arbitrary angles (Fig. 21). The high-frequency properties of metals in a magnetic field are an inexhaustible source of information about conduction electrons. Cyclotron resonance⁵² is undoubtedly the most popular effect, whose origin will be clear from an inspection of Fig. 22. If the time interval T_H between successive reentry of the belt by the electrons in a magnetic field parallel to the boundary is a multiple of the field period $T_\omega = 2\pi/\omega$,

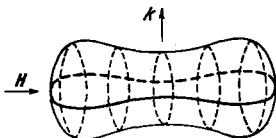


FIG. 21. Electron paths (broken lines) intersecting a belt (thick line).

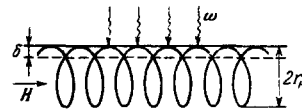


FIG. 22. When the constant magnetic field is parallel to the surface of the metal, so that the electrons are returned to the skin layer ($\delta \ll r_H \ll l$), cyclotron resonance can be observed.

then resonance between electrons and the wave will ensure that the conductivity will become infinite for $\tau \rightarrow \infty$ and the impedance will vanish. On the other hand, the period $T_H = 2\pi/\omega_c$ [$\omega_c = eH/m^*c$, $m^* = (1/2\pi)\partial S(\epsilon, p_x)/\partial \epsilon$] is different for different electrons. Because of degeneracy, the effect is determined by Fermi electrons, i.e., electrons with $\epsilon = \epsilon_F$ undergo resonance. The selection of electrons in accordance with p_x is connected with the presence of extrema in the dependence of $m^* = m^*(\epsilon_F, p_x)$ on p_x . The dependence on the longitudinal momentum component near the extrema is less important than for other values of p_x . In fact, the extremal values of the effective mass $m_j^* = m^*(\epsilon_F, p_{x,j}^{ext})$ determine the resonance conditions:

$$\omega = n \frac{eH}{m_j^* c}, \quad n = 1, 2, 3, \dots \quad (19)$$

Thus, cyclotron resonance is a direct method for the experimental determination of the extremal effective mass of conduction electrons. Cyclotron resonance was first discovered experimentally by Fawcett⁵³ in the case of tin and copper. It eventually evolved into a standard method for measuring the effective masses of conduction electrons,⁵⁴ which is a necessary stage in the interpretation of the electron energy spectrum.

The importance of cyclotron resonance lies not only in the particular results that it yields, but also in that it has drawn attention to the electrodynamics of metals in magnetic fields. Thus, it has always been considered that the main optical property of a metal is its ability to reflect electromagnetic waves and that, as soon as it begins to transmit such waves (for $H = 0$), it is not very different from a dielectric. At frequencies greater than the plasma frequency of the electrons in a metal, the dielectric permittivity of the metal is positive and absorption is a consequence of the interband internal photoelectric effect.

The discovery of cyclotron resonance has led to a radical change in our picture of the interaction between conduction electrons and the electromagnetic field. It turns out that a strong enough magnetic field can substantially modify the propagation of electromagnetic waves in metals and, to some extent, "eliminate" the skin effect, transforming oscillations whose amplitude falls by a factor of $e^{-2\pi}$ over one wavelength into weakly attenuated waves with $\text{Im}k \ll \text{Re}k$. Weakly attenuated waves in metals are not merely a fanciful idea: many of them have in fact been verified experimentally (see, for example, Ref. 55).

Many waves have no direct connection with cyclotron resonance. Neither their properties nor even an enumeration of them form part of our task here. We shall confine our attention to some simple examples demonstrating the role of the magnetic field.

D. Low-frequency elliptically polarized wave—the helicon

The helicon⁵⁶ can propagate through metals with different numbers of electrons and holes ($n_1 \neq n_2$) along a sufficiently strong magnetic field H .

The dispersion relation for helical waves is

$$\omega = \frac{ck^2 H \cos \theta}{4\pi e(n_1 - n_2)}, \quad \omega\tau \ll 1, \quad (20)$$

where θ is the angle between the wave vector \mathbf{k} and the magnetic field H . The wave is not attenuated because the Hall components of conductivity are much greater than dissipative components (which, of course, are transverse) in the case of metals with $n_1 \neq n_2$ in a strong magnetic field. The attenuation length for a helical wave is determined either by collisional mechanisms (i.e., σ_{xx} and σ_{yy}) or by collisionless mechanisms (here again, we have the belt).

E. High-frequency magnetic plasma wave

When $\omega\tau \gg 1$ and $k r_H \ll 1$, a weakly attenuated magnetic plasma wave⁵⁷ can propagate in a compensated metal ($n_1 = n_2$) in a strong magnetic field ($\omega_c \gg \omega \gg 1/\tau$). In the simplest case, the dispersion relation for the magnetic plasma wave is the same as for the celebrated Alfvén wave:

$$\omega = v_a k, \quad v_a = \frac{H}{\sqrt{4\pi n \bar{m}^*}},$$

where v_a is the Alfvén velocity (\bar{m}^* is a combination of the effective masses of the electrons and holes).

The dispersion relation for the magnetic plasma wave can readily be derived by a simple hand-waving argument if we note that the frequency ω always appears together with τ in the form $\tau/(1 - i\omega\tau)$, and the transition from $\omega = 0$ to $\omega\tau \gg 1$ means that τ is replaced by i/ω . The effective permittivity of the metal electrons is $\epsilon = 4\pi i\sigma/\omega$, and the dispersion relation for the wave is $\omega^2 = c^2 k^2/\epsilon$. When $H = 0$, $\sigma = ne^2\tau/m^*$, and the replacement $\tau \rightarrow i/\omega$ leads to negative permittivity, i.e., the wave cannot propagate ($\epsilon = -\omega_L^2/\omega^2 < 0$; where $\omega_L = \sqrt{4\pi ne^2/m^*}$ is the plasma frequency). When $\omega_c\tau \gg 1$, the dissipative transverse conductivity is $\sigma \approx (ne^2\tau/m^*)(\omega_c\tau)^{-2}$ and the replacement $\tau \rightarrow i/\omega$ leads to positive permittivity, ensuring propagation of the wave.⁷⁾ The Hall components of the conductivity tensor play a secondary role because the number of electrons and holes is the same.

F. Dopplersons, cyclotron waves, and anisotrons

The spatial and temporal dispersion of conductivity (the dependence of $\hat{\sigma}$ on the wave vector \mathbf{k} and frequency ω) play a minor role for the two waves considered above. However, as the mean free path increases with

⁷⁾Of course, this is not accidental: when $H = 0$, the field frequency ω is higher than the resonance frequency ω_R (which, in this case, is zero!) and, when $H \neq 0$, the field frequency ω is lower than the resonance frequency ω_R , which is then equal to ω_c (see above). Having outlined the resonance function $\epsilon = \epsilon(\omega)$, we can readily see the reason for the difference between these two limiting cases.

decreasing temperature, and the magnetic field is reduced (i.e., with increase in $\omega\tau$, kl and/or kr_H) the spatial and temporal dispersion of conductivity assume a dominant role in establishing the function $\omega = \omega(k)$ for the weakly attenuated waves in metals.⁵⁵ Thus, helicons and magnetic plasma waves transform into dopplersons,⁵⁸ cyclotron waves,⁵⁵ anisotrons,⁵⁹ and so on, as the wave number increases. In many cases, they transform into the extensively-studied boson quasiparticles. In the terminology of the electrodynamics of media with spatial dispersion,⁶⁰ they are all additional macroscopic waves because their wavelength is much greater than the interatomic distance ($ka \ll 1$).

It is important to emphasize (and this is part of our theme in this review) that the limiting values of the components of σ_{ik} for $k \rightarrow \infty$ are very dependent on the geometry of the Fermi surface. This is very clear, for example, from the expression for the transverse components of σ_{ik} in zero magnetic field when $kl \gg 1$ ($\omega\tau \approx 1$):

$$\sigma_{\alpha\beta} = \frac{e^2}{8\pi^2 \hbar^3 k} \oint_{(F)} v_\alpha v_\beta \delta(nv) dS, \quad (21)$$

$$\mathbf{v} = \frac{\mathbf{v}}{v}, \quad \mathbf{n} = \frac{\mathbf{k}}{k}, \quad n_z = 1, \quad \alpha, \beta = x, y.$$

The structure of the last equation is very similar to that of (18) which gives the absorption coefficient for short-wave sound.

It is clear from the above formula that, when there is no magnetic field and $kl \gg 1$, conduction is determined by electrons responsible for the collisionless Landau damping ($\mathbf{v} \cdot \mathbf{n} = 0$). The situation changes radically in a magnetic field: weakly-attenuated waves can exist only when they fall into the "transparency windows" within which there is no collisionless damping. In the great majority of cases, the weakly-attenuated waves exist near the damping boundary on which $\hat{\sigma}$ has a singularity, and it is this proximity to the boundary that makes the contribution of electrons to the dispersion relation of the wave particularly important.⁶¹

G. Sound in a magnetic field

The influence of the magnetic field on conduction electrons can, of course, also be seen in the electronic part of the sound absorption coefficient. Sound penetrates metals relatively readily, so that studies of the propagation of sound in metals are important for the interpretation of the electron energy spectrum.

The analog of (18), which will describe the absorption of sound in a magnetic field, can be written in the form given below, where the magnetic field is perpendicular to the wave vector of the sound wave and $1 \ll \omega_c\tau \ll kl$. The "geometry" of the of the interaction between the electron and sound wave is clearly seen from Fig. 21: as the number of times the electron crosses the belt increases, the sound absorption coefficient increases. The leading term in Γ_e has a particularly simple form⁶²

$$\Gamma_e(H) \approx \Gamma_e^{\text{mon}} = \frac{2\omega}{(2\pi\hbar)^3 \rho_s} \oint_{(F)} 2\pi\omega_c \bar{\tau} |\Lambda|^2 \frac{dS}{v^3} \delta(nv), \quad (22)$$

where $\bar{v} = 1/\bar{\nu}$, and $\bar{\nu}$ is the relaxation frequency ($\nu = 1/\tau$), averaged over the period of revolution in the mag-

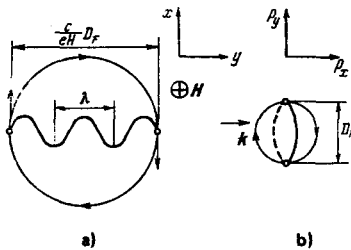


FIG. 23. Origin of Pippard oscillations in the sound absorption coefficient. The amplitude of the oscillations depends on electrons lying near the ends of the extremal diameters where the electron velocity lies in a plane of equal phase of the sound wave: a)—in r -space; b)—in p -space.

netic field.

However, the term in $\Gamma_e(\mathbf{H})$ is of much greater interest but is, unfortunately, smaller than this by a factor of $\sqrt{k\gamma_H}$ and contains a periodic dependence on the magnetic field:

$$\Gamma_e(H) = \Gamma_e^{\text{mon}} + \Gamma_e^{\text{osc}}, \quad (23)$$

$$\Gamma_e^{\text{osc}} \approx \Gamma_e^{\text{mon}} \frac{1}{\sqrt{k\gamma_H}} \sum_m \sin\left(\frac{ck}{eH} (\Delta p_y)_m \pm \frac{\pi}{4}\right).$$

The sum in the above expression is evaluated over all the extremal diameters of the Fermi surface (Figs. 23 and 26). It is clear that Γ_e is a periodic function of the reciprocal of the magnetic field, and the periods $\Delta(1/H)$ are determined by the extremal projections of the diameters onto the direction perpendicular to both \mathbf{k} and \mathbf{H} (we recall that $\mathbf{k} \perp \mathbf{H}$; see Fig. 23):

$$\Delta \frac{1}{H} = \frac{2\pi e}{ck (\Delta p_y)_m}.$$

The origin of the periodic dependence is quite clear: the situation repeats itself whenever the number of waves that can be fitted into the orbit diameter changes by one [see (23)]. The periodic form of $\Gamma_e(\mathbf{H})$ is often referred to as the Pippard or geometric resonance. The amplitude of the Pippard resonance is determined by electrons lying near the points at which the path of the electron with the extremal projection of the reference diameter crosses the "belt"; the remaining electrons are found to be ineffective (see Fig. 23). By rotating the magnetic field \mathbf{H} and the wave vector \mathbf{k} , these points can be made to move over the Fermi surface, so that its geometry can be investigated in detail. The interaction between electrons and a sound wave in a magnetic field is the source of many other resonance phenomena. They are, in fact, referred to as magnetoacoustic phenomena. They depend essentially on the geometry of the experiment and on the geometric properties of the Fermi surface. Here, we shall consider one of the magnetoacoustic resonances that arises in

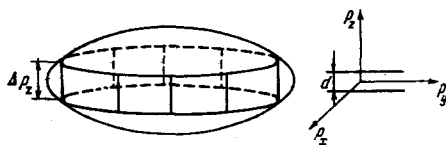


FIG. 24. Quantization of chords segregates electrons lying on lines on the Fermi surface. The two lines are shown, corresponding to a quantized value of the chord length $\Delta p_y = n\pi \hbar/d$, where d is the plate thickness and n is an integer.

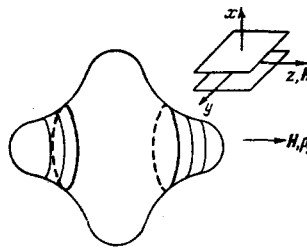


FIG. 25. If $D_{\text{lim}}^y c/eH > d$, a plate of thickness d can contain orbits smaller than a given orbit (the latter is defined by $D_{\text{lim}}^y c/eH = d$ and is shown by the thick line); orbits between the limiting positions do not fit into the plate at all.

metals with open Fermi surfaces.⁶³

If the period of the motion along an open path is equal to the wavelength of the sound wave, we observe a resonance interaction between electrons and the sound wave. This leads to a periodic dependence of the sound absorption coefficient on the reciprocal of the magnetic field. The resonance condition can easily be derived from the connection between paths in p - and r -spaces. If the wave propagates at right-angles to the magnetic field $\mathbf{H}(H_x = H_y = 0; H_z = H)$ and in the direction in which p_x is open, the period of the absorption coefficient is

$$\Delta \frac{1}{H} = \frac{2\pi e}{ck} \frac{1}{2\pi \hbar b_x},$$

where b_x is the smallest period of the reciprocal lattice along the p_x axis.

6. ELECTRONS COLLIDING WITH BOUNDARIES

The impact of electrons on the specimen surface has long been attracting the attention of workers concerned with the electronic properties of metals. As far back as 1938, Fuchs⁶³ reported a theoretical study of the resistance of a thin plate as a function of its thickness and formulated a phenomenological boundary condition describing partially specular reflection of electrons by the boundary. It seemed for a long time that any boundary within a metal was rough, i.e., it resembled a diffuse reflector for Fermi electrons with wavelengths of the order of the interatomic separation. An electron should be reflected diffusely at a surface of this kind (that was the belief).

In the case of diffuse reflection of electrons by the surfaces of the specimen, the conductivity of the plate (if, of course, its thickness d is much less than the mean free path l) is governed exclusively by electrons moving parallel to the plate surface. They lie on the belt $\mathbf{v}_F \cdot \mathbf{n} = 0$, where \mathbf{n} is the normal to the plate surface.⁶⁴ It is interesting to note that the specific conductivity $\sigma(d)$ of the plate for $d \ll l$ increases logarithmically with increasing bulk mean free path $[\sigma(d)]$

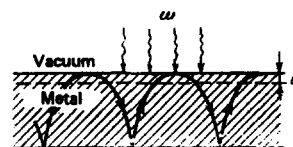


FIG. 26. Electron returns to the skin layer after reflection from the back surface of the plate.

$\sim \ln(l/d)$. This distinguishes the static conductivity of a thin plate from the limiting anomalous skin effect ($\sigma \ll l$) in which the impedance is determined by the collisionless limit of the specific conductivity tensor (21). The exceptional role of the "belt" electrons (or, more precisely, the ineffectiveness of all other electrons) ensures that the conductivity of thin films is a phenomenon that is very sensitive to the geometry of the Fermi surface.

Now that we have considered theoretical studies of the conductivity of thin films and wires, we must note that it is not always as easy as it might appear from the above examples to identify the effective electrons, i.e., the electrons responsible for a particular effect. For example, the conductivity of thin cylindrical wires, whose radius is much smaller than the mean free path and whose boundary reflects diffusely, is not exclusively determined by electrons moving along the axis of the wire. In fact, the conductivity includes contributions due to all the Fermi electrons.⁶⁵

The pressure of experimental evidence has led, eventually, to the realization that electrons are very often reflected specularly from the metal surface.⁶⁶ For an electron with an anisotropic dispersion relation, this means that not only the energy but also the quasimomentum component parallel to the surface are conserved [$p_{\parallel} = p - (\mathbf{p} \cdot \mathbf{n})\mathbf{n}$, where \mathbf{n} is the normal to the surface], whereas the normal component of the velocity $\mathbf{v} \cdot \mathbf{n}$ changes sign.

The interaction between an electron with a complicated dispersion relation and the surface of the specimen leads to a peculiar complication in a number of commonplace properties. For example, it is well known that the components of momentum are quantized in an infinitely deep potential well, whereas chords are quantized in the case of an electron with a complicated dispersion relation⁶⁷ (Fig. 24), and this means that the picture of the electronic subbands of metal plates is very unusual. Once the quantum-mechanical size effect⁶⁸ was discovered, this phenomenon ceased to be theoretically exotic.

The most direct demonstration of the specular reflection of electrons from the specimen surface was undoubtedly the discovery of oscillations due to surface levels occupied by electrons in the magnetic field, which was made by Khaikin.⁶⁹ The motion of an electron which has been reflected specularly from the surface of a metal in a magnetic field, (Fig. 12) is the sum of two motions, namely, infinite motion along the surface and finite (periodic) motion along the normal to the surface. The latter motion is quantized, so that discrete surface levels appear and give rise to oscillations in the surface impedance as a function of the applied magnetic field. The complete theoretical explanation of this phenomenon is due to Nee and Prange.⁷⁰

A single surface is sufficient for the Khaikin oscillations to appear. When the electrons interact with the two surfaces of a plate of thickness d (d and r_H must then, of course, be much smaller than the mean free path l), peculiar resonance size effects become possible

and can easily be described in terms of the geometric language.

Out of all the possible orbits, the plate isolates the one that fits into it (Fig. 25). Resonance should be observed for this orbit⁷¹ and, has, in fact, been found in bismuth.⁷² It was used to investigate nonextremal sections through the Fermi surface, which deserve particular attention.

The mechanisms responsible for returning the electrons to the skin layer may, in addition to the magnetic field, include a contribution due to reflection from the other surface of the specimen (Fig. 26). If $\delta \ll d$ and $r_H \ll l$, cyclotron resonance can also be observed for such orbits.

7. CROSSING OF THE FERMI SURFACE BY ITS SHIFTED ANALOG, AND MIGDAL-KOHN SINGULARITIES

The singularity in the dependence of phonon energy on quasimomentum (Migdal-Kohn singularity⁷⁴), which arises from the interaction between phonons and electrons in metals, is due to the nonuniform filling of \mathbf{p} -space with electrons and has a clear geometric meaning. Since, by virtue of the Kramers-Kronig relationships, singularities in $\text{Re}\omega(\mathbf{q})$ produce singularities in $\text{Im}\omega(\mathbf{q}) = \Gamma_{\mathbf{q}}$ and vice versa, and since integrals containing δ -functions are easier to handle than integrals defined as principal values, the geometry of singularities in phonon \mathbf{q} -space can be established by using the expression for the reciprocal phonon lifetime $\Gamma_{\mathbf{q}}$ (\mathbf{q} is the quasimomentum) due to electron-phonon collisions:

$$\Gamma_{\mathbf{q}} = \int |M|^2 \{n_F(\epsilon_p) - n_F(\epsilon_p + \hbar\omega_{\mathbf{q}})\} \delta(\epsilon_p + \hbar\omega_{\mathbf{q}} - \epsilon_{p+\mathbf{q}}) d^3p, \quad (24)$$

where $n_F(\epsilon)$ is the Fermi function and the transition matrix element M includes all factors. At absolute zero, the difference between the Fermi functions selects the region in \mathbf{p} -space bounded by the surfaces $\epsilon_p = \epsilon_F$ and $\epsilon_p = \epsilon_F - \hbar\omega_{\mathbf{q}}$ (Fig. 27a). The singularities in $\Gamma_{\mathbf{q}}$ are connected with a change in the structure of the region of integration which is defined by the intersection of the surface $\epsilon_p + \hbar\omega_{\mathbf{q}} = \epsilon_{p+\mathbf{q}}$ with the surfaces $\epsilon_p = \epsilon_F$ and $\epsilon_p = \epsilon_F - \hbar\omega_{\mathbf{q}}$. Since $\hbar\omega_{\mathbf{q}} \ll \epsilon_F$, we can expand the expression in (24) in powers of $\hbar\omega_{\mathbf{q}}$, so that

$$\Gamma_{\mathbf{q}} \approx \hbar\omega_{\mathbf{q}} \int |M|^2 \delta(\epsilon_p - \epsilon_F) \delta(\epsilon_{p+\mathbf{q}} - \epsilon_F) d^3p. \quad (25)$$

We have omitted $\hbar\omega_{\mathbf{q}}$ from the δ -function describing conservation of energy and replaced ϵ_p with ϵ_F . The region of integration in (25) is the line of intersection of the Fermi surface with its analog shifted by $-\mathbf{q}$. A change in the topology of this line (in particular, its vanishing) produces a singularity in $\Gamma_{\mathbf{q}}$. The Migdal-Kohn singularity⁷⁴ is due to the vanishing of the line of intersection at $q = D_F$ (Fig. 27b), and the nature of the singularity depends on how the surfaces touch at $q = D_F$ (see Refs. 75 and 76; the last paper predicts an enhancement of the Migdal-Kohn singularities for Fermi surfaces containing finite cylindrical and flat segments).

If the Fermi surface splits into several parts, the singularity should still be observed at the value of the phonon quasimomentum \mathbf{q} at which one part of the Fer-

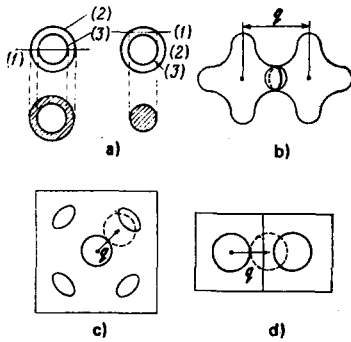


FIG. 27. a—Phonon absorption is due to electrons on a segment of the surface $\epsilon_p + \hbar\omega_q = \epsilon_{p+q}$ (1) lying between the surfaces $\epsilon_p = \epsilon_F$ (2) and $\epsilon_p = \epsilon_F - \hbar\omega_q$ (3); the shape of the segment of p-space on which electrons interacting with photons are located depends on the magnitude of q (for simplicity, we show a spherical Fermi surface). Approximate analysis: b—electrons absorb phonons if the Fermi surface and its analog shifted by $-q$ intersect (the line of intersection is shown by the thick line in the figure); c—when the phonon momentum q is large enough, the Fermi-surface cavity will cut another when it is shifted; d—the Fermi surface intersects its analog in a neighboring cell.

mi surface shifted by $-q$ touches another part on the unshifted surface (Fig. 27c). Further increase in q produces a sudden increase in the absorption coefficient and $\text{Re}\omega$ should have a singularity with opposite sign as compared with the Migdal-Kohn singularity.⁷⁴ Observation of such singularities could be a means of measuring the separation between individual pieces of the Fermi surface.

For the free electron gas, the geometric locus of Migdal-Kohn singularities is a sphere of radius $2p_F$. However, for real spherical Fermi surfaces such as those of sodium, potassium, rubidium, and cesium, the situation must be more complicated: the possibility of umklapp processes (in other words, the periodicity of Γ_x with the period of the reciprocal lattice, i.e., $\Gamma_{q+2\pi\hbar} = \Gamma_q$) ensures that Γ_q exhibits singularities when the shifted sphere touches the spheres in the neighboring cells (Fig. 27d). This phenomenon should be observed in metals with Fermi surfaces of any kind and may be useful in locating the Fermi surface in reciprocal space.

8. CROSS SECTIONS AND BELTS MODIFY THE TOPOLOGY

Shoenberg and Templeton⁷⁷ investigated the de Haas-van Alphen effect and found that the amplitude of the oscillations increased substantially for a particular direction of the magnetic field H . This was explained by them by saying that, for this direction of the magnetic field, both $\partial S/\partial p_x$ and $\partial^2 S/\partial p_x^2$ vanish, so that the expansion of S in powers of Δp_x begins with the fourth-order term and it is this that produces the increase in amplitude. The small factor $\sqrt{\hbar\omega_c}/\epsilon_F$ is replaced with the larger factor $(\hbar\omega_c/\epsilon_F)^{1/4}$. It is clear that, for this direction of H , there is a change in the character of the extremum in p_x on the section of the Fermi surface. Figure 28 shows the functions $S(\epsilon_F, p_x)$ for different directions of H (the dumbbell is taken as an example) and

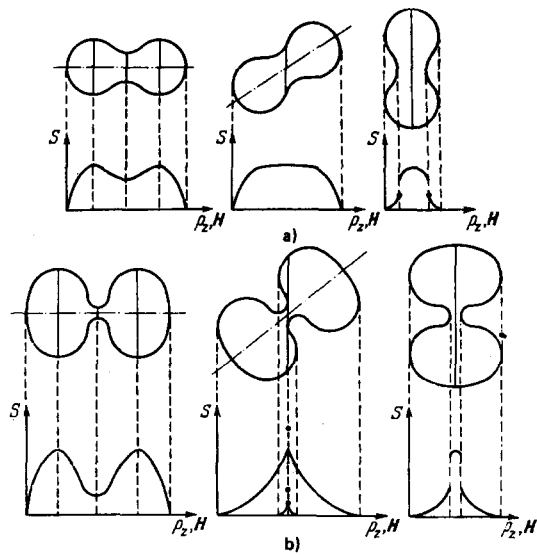


FIG. 28. Cross-sectional area of the Fermi surface as a function of p_x for different directions of the magnetic field: a—dumbbell with thick neck; b—dumbbell with thin neck.

the variation in the sections (including their number and position). This variation would not be possible for a convex Fermi surface.

The structure of the section may also vary in a more complicated way as compared with Fig. 28a. If there is a direction in which one of the extremal cross sections contains a self-crossing point, the variation in the structure of the cross sections and hence in the spectrum of the de Haas-van Alphen oscillations occurs in a more complicated way (Fig. 28b), and the amplitude of the critical oscillation (corresponding to a figure-eight cross section) is anomalously low. This problem has not, however, been extensively investigated.⁸⁾

The question of singularities in the phonon spectrum of metals due to topologic changes in the structure was investigated relatively recently.⁷⁹⁻⁸¹ Let us turn to Fig. 19. It is clear that the number of belts is different for different directions of the wave vector. This means that there is a direction $n = n_c$ for which the belt changes its structure (in Fig. 19, it contains a point of self-intersection). Figure 29 shows a piece of the Fermi surface resembling a hill (we have referred to it as a

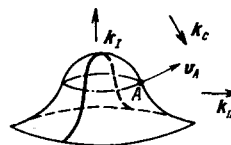


FIG. 29. Origin of belts at the point A on a line of parabolic points for $\mathbf{k} = \mathbf{k}_0 + \mathbf{v}_A$ (Fermi-surface hill). When $\mathbf{k} = \mathbf{k}_1$, there is no belt; the belt corresponding to $\mathbf{k} = \mathbf{k}_{11}$ is shown by the thick line.

⁸⁾ Azbel⁷⁸ has investigated oscillations connected with nonextremal cross sections with self-intersection and has shown that their amplitude is lower by a factor of $\epsilon_F/\hbar\omega_c$ as compared with the amplitude due to the extremal cross section without self-intersection.

puckered plane¹⁹). There is a two-dimensional region of directions for which there is no belt at all but, for directions outside this region, the belt does exist. When a direction belonging to the region in which there is a belt approaches the critical direction, $\mathbf{n} - \mathbf{n}_c$, the belt assumes the shape of a small ellipse which contracts to a point at $\mathbf{n} = \mathbf{n}_c$. If we suppose that the velocity of electrons on the belt is perpendicular to the wave vector (we neglect the velocity of sound in comparison with the Fermi velocity), the critical points⁹) lie on the lines of parabolic points, i.e., on lines of zero Gaussian curvature K of the Fermi surface which, as we have noted, is a necessary attribute of surfaces with dents, necks, and so on.

Analysis of the structure of the belts given by (16) and (17) shows that hyperbolic points can be of two types, referred to as O - and X -points.⁷⁹ At O -points, the belt just appears whereas, at X -points, the belt has a self-intersection. The existence of parabolic points on the Fermi surface, and hence of critical directions for the propagation of sound, should lead to singularities in the angular dependence of the sound absorption coefficient and other transport coefficients (for example, the electrical conductivity tensor in the presence of large spatial dispersion).

The above phenomenon corresponds to a relatively rare situation in which the geometry of the Fermi surface (geometry at the point) affects (or, more precisely, should affect) macroscopically observable phenomena for $H=0$. It is important to emphasize that (18) is constructed so that the contribution of the neighborhood of the singular point to Γ_0 is of the same order as, or logarithmically greater than (!), that due to the remainder of the surface.¹⁰) Figure 30 shows the structure of the singularities in $\Gamma_0 = \text{Im}\omega$ and $\text{Re}\omega$ for O - and X -points. The existence of pairs of closely spaced singularities is connected with the presence for each singular point of the "antipod" point with antiparallel

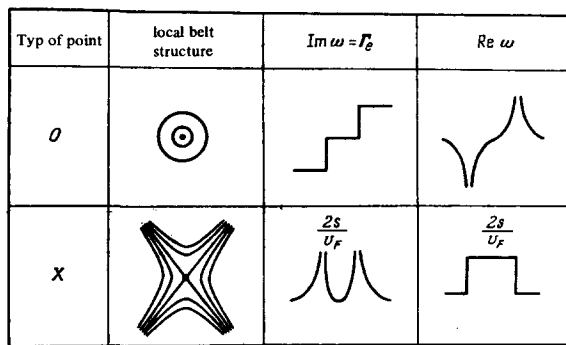


FIG. 30. Nature of angular $\text{Im}\omega$ and $\text{Re}\omega$ singularities due to O - and X -points. The separation between pairs of singularities is $\approx 2s/v_F$.

⁹)The point of self-intersection of the critical belt on the surface of a dumbbell (see Fig. 19); the point to which the elliptical belts contract (see Fig. 29).

¹⁰)The formula for the components of the conductivity tensor (21) for $kl \gg 1$ is, as already noted, similar in structure to (18) (see Refs. 44 and 47).

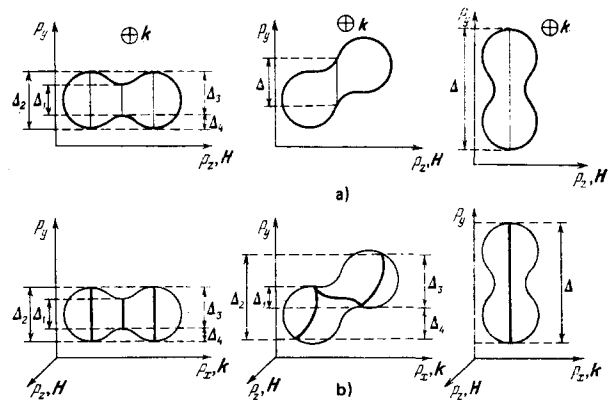


FIG. 31. The spectrum of Pippard oscillations is different for different directions of the magnetic field H and wave vector \mathbf{k} : the frequencies are determined by the quantities $\Delta \beta_{\text{extr}} \equiv \Delta_f$. a—when \mathbf{k} is fixed, the belt (solid line) does not change, but the oscillation spectrum does, $H \parallel p_x$; b—the change in the topology of the belt for fixed H will also produce a change in the oscillation spectrum. The extremal trajectories are shown by thin lines.

velocity (this is a consequence of the symmetry of the Fermi surface under the replacement of \mathbf{p} with $-\mathbf{p}$). As $s/v_F \rightarrow 0$, the critical directions associated with the antipoles are found to coincide. The $\text{Re}\omega$ singularities extinguish one another, but the $\text{Im}\omega$ singularities add.

The absorption of sound in a magnetic field for intermediate fields $1 \ll \omega_c \ll kl$ and $\mathbf{k} \perp \mathbf{H}$ should also exhibit singularities connected with changes in the topology of

TABLE II. Dependence of the amplitude and phase of the oscillating part $\Gamma_0(H)$ on the type of points of intersection of a "belt" with an extremal trajectory, and experimental geometry.

Points	Elliptic (both)	One elliptic, the other parabolic, X -type
Amplitude	$\Gamma_e \frac{\omega_c \tau}{(kr_H)^{1/2}}$	$\Gamma_e \frac{\omega_c \tau}{(kr_H)^{1/2}}$
Phase	$+\frac{\pi}{4}$	0
Points	Both X -type parabolic	Both X -type parabolic
Amplitude	$\Gamma_e \frac{\omega_c \tau}{(kr_H)^{1/2}}$	$\Gamma_e \frac{\omega_c \tau}{(kr_H)^{1/4}}$
Phase	$-\frac{\pi}{4}$	$\frac{\pi}{8}$

the belt. Comparison of (18) and (22) will show that, insofar as the leading term is concerned (i.e., the term that depends monotonically on H), Γ_e^{mon} has the same singularities as Γ_e at $H=0$. The oscillating part is more interesting. The oscillation spectrum depends on the direction of propagation of sound and on the direction of the magnetic field. Both the periods and their number depend on direction (Fig. 31). As critical directions are approached, i.e., directions in which the oscillation spectrum is modified, this should give rise to similar periods, so that combinations of the corresponding harmonics produce beats. It is clear that, from the experimental point of view, it is easiest to detect an increase in the oscillation amplitude connected with the fact that electrons responsible for the Pippard amplitudes lie near points at which the Fermi surface become flat. The points in which we are interested are the points of intersection of the "belt" with the orbit of the electron that has the extremal projection of the reference diameter. It is clear that the point of intersection can be made to coincide with the point at which the Fermi surface is flat either by varying the direction of propagation or of the magnetic field. The geometry of possible experiments (directions of H and q) and the theoretical predictions^{79,80} can be seen in Table II.

9. SLOW ELECTRONS

Conduction electrons are the fastest quasiparticles in metals. Their velocity exceeds the phonon velocity by a factor of many thousands. This is why the thermal conductivity of metals is much higher than the thermal conductivity of dielectrics, and many properties of metals can be investigated without bringing the motion of ions into the discussion. Nevertheless, not all the electrons in the metal, not even those whose energy is equal to ε_F , move with the same velocity. The complicated form of the dispersion relation $\varepsilon = \varepsilon(p)$, including its anisotropy, ensures that electrons located at different points on the Fermi surface have different velocities.

It is interesting to note that slow electrons play a very appreciable role in many properties of a metal, i.e., the relative contribution of electrons increases with decreasing velocity. This can be explained as follows. As we have frequently noted, most of the electronic characteristics of a metal are described by formulas containing integrals over the Fermi surface. If these integrals can be written in the form $\oint_{(F)} (ds/v^\alpha) F$, and the function F at points on the Fermi surface varies slowly with v , the exponent α is a measure of the relative participation of slow electrons.⁸² Indeed, it turns out that frequently α is greater than zero. In Table III, formulas describing several effects are arranged in order of increasing α .

It is important to emphasize that the electron mean free path l in these formulas is a slowly-varying function of velocity. This is clear from the approximate expressions for it (see Ref. 83, Chap. 7): in the case of scattering by screened impurities

$$l^{-1} \approx N s_a,$$

TABLE III. Contribution of slow electrons to properties of metals.

Electrical conductivity of metal*	$\sigma_{ik} = \frac{2e^2}{(2\pi\hbar)^3} \oint_{(F)} l n_i m_k dS, \quad \alpha=0$
Number of electron states on the Fermi surface per unit volume (determines the thermodynamics of the electron gas)	$\nu(\varepsilon_F) \equiv \nu_F = \frac{2}{(2\pi\hbar)^3} \oint_{(F)} \frac{dS}{v}, \quad \alpha=1$
Sound absorption coefficient of electrons ($H=0$)	$\Gamma_e = \frac{2\omega}{(2\pi\hbar)^3 \rho s^3} \oint_{(F)} l \Lambda ^2 \frac{dS}{v^3} F(n \cdot \nu), \quad \alpha=2$
Monotonic part of the sound absorption coefficient in a magnetic field ($kl \gg \omega_c \tau \gg 1, k \perp H$)	$\Gamma_e^{\text{mon}} = \frac{4\pi\omega}{(2\pi\hbar)^3 \rho s^3} \oint_{(F)} \omega_c l \Lambda ^2 \frac{dS}{v^3} \delta(n \cdot \nu), \quad \alpha=3$
Acoustoelectric current due to current of coherent phonons	$J_A = \frac{2\pi e W \omega}{(2\pi\hbar)^3 \rho s^3} \oint_{(F)} l \Lambda ^2 \frac{\partial^2 \varepsilon}{\partial p_n^2} \frac{dS}{v^3} \delta(n \cdot \nu), \quad \alpha=3$

*In the case of electronic thermal conductivity, κ , the parameter α is also zero.

where N_{imp} is the number of impurity atoms per unit volume and, in the case of scattering by phonons,

$$l^{-1} \approx N s_a \frac{T}{M s^2} \left(\frac{T}{\theta} \right)^4 \int_0^{\theta/T} \frac{4x^4 dx}{e^x - 1},$$

where N is the number of metal ions per cm^3 , M is the ion mass, θ is the Debye temperature, and s_a is of the order of the effective scattering cross-section of an atom ($s_a \approx a^2$). Both the last formulas and the formulas in Table III are valid in the limit of the degenerate electron gas ($T \ll |\varepsilon_n - \varepsilon_n|$). Moreover, the adiabatic approximation demands that the velocity of electrons participating in these effects be greater than the velocity of sound, s . However, in comparison with electron velocities, $\sqrt{T/m}$ and s are so small that, as they are approached, the effect becomes substantially enhanced (or suppressed).

The last line of Table III gives the expression for the acoustoelectric current J_A excited in a metal by a beam of coherent phonons of power W and frequency $\omega = \omega(k)$. The appearance of this current is due to the same interaction between phonons and metal electrons that is responsible for the attenuation of sound in accordance with Eqs. (18), (22), and (23). When electrons absorb phonons, the latter transfer their momenta to the electrons and, in the final analysis, this is responsible for the acoustoelectric effect. As always, the condition $kl \gg 1$ discriminates against all electrons other than those in the "belts"⁸⁴ and the factor $\partial^2 \varepsilon / \partial p_n^2 = (m_n^*)^{-1}$ is a consequence of the "transformation" of the transferred phonon momentum into a change in the electron velocity:

$$\Delta v_i = \frac{\partial v_i}{\partial p_k} \Delta p_k = \hbar k \frac{\partial^2 \varepsilon}{\partial p_n^2},$$

where m_n^* is the effective mass in the direction of $k = k\mathbf{n}$. The anomalously large contribution of slow electrons becomes particularly noticeable when we con-

sider the contribution of electrons in a small piece of the Fermi-surface to the different properties of metals. For simplicity, we suppose that this piece is a sphere. We shall assume that the number of electrons in the piece is n_a , so that, in accordance with Table III,

$$\sigma, \kappa \propto n_a^{2/3}, \quad v_F \propto n_a^{1/3}, \quad \Gamma_e \propto \text{const}, \quad \Gamma_e^{\text{mon}}, \mathbf{H}, J_A \propto n_a^{-1/3}.$$

Of course, we can go to the limit as $n_a \rightarrow 0$ in all the above formulas. It follows from the condition $\varepsilon_{F_a} \gg T$ and $v_F > s$ that

$$n_a \gg \frac{1}{a^3} \left(\frac{T}{\varepsilon_a} \right)^{3/2}, \quad \frac{1}{a^3} \frac{ms^2}{\varepsilon_a}, \quad \varepsilon_a = \frac{\hbar^2}{a^2 m}.$$

However, since T and ms^2 are very small in comparison with ε_a , the increase in the acoustoelectric current and the sound absorption coefficient in a magnetic field with decreasing number of electrons in the Fermi-surface piece should be observable.

10. THE FERMI SURFACE CHANGES ITS GEOMETRY

Phase transitions of the crystal lattice of metals occur under external disturbances or as a result of a change in the temperature. This is accompanied by a change in the Fermi surface and hence in all the electronic properties of metals. The many phase transitions include those in which the electronic subsystem of the metal plays the leading role (examples are transition to the superconducting or ferromagnetic state and the metal-dielectric transition). However, even in these cases, the Fermi surface necessarily "feels" the transition: in the case of a transition to the superconducting state, a small energy gap opens at $\varepsilon \approx \varepsilon_F$ and makes the superconducting state stable, whereas, in the case of a transition to the ferromagnetic state, the Fermi surface splits into two because of the lifting of degeneracy in electron spin; the Fermi surface vanishes altogether in the course of the metal-dielectric transition.

A phase transition (especially of the second kind) is a complicated phenomenon accompanied, as a rule, by a change in symmetry, an increase in fluctuations, hysteresis, and so on. The change in the geometry of the Fermi surface and its manifestations is, in most cases, secondary. Within the framework of the present review, it will therefore be natural to confine our attention to those changes in the geometry of the Fermi surface that are not accompanied by phase transitions.

In metals under pressure, the accompanying change in interatomic separations modifies the entire energy structure of the metal. However, if there is no change in the symmetry of the body, or of no isomorphous phase transition takes place, all the changes are quantitative rather than qualitative up to some critical pressure p_c . A qualitative change without phase transition can occur by changing the Fermi surface. In \mathbf{p} -space, each electron energy band has points $\mathbf{p} = \mathbf{p}_k$ at which the connectivity of the equal-energy surfaces changes: either a hole is produced (vanishes) on the equal-energy surface or a neck is "broken" (formed) (Fig. 32). At energies ε_k at which the connectivity of the equal-energy surfaces undergoes a change, the density of electron states $\nu(\varepsilon)$ has a van Hove-type singularity⁴² because

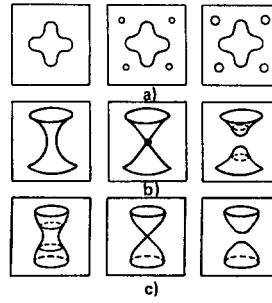


FIG. 32. Change in the connectivity of the Fermi surface under a phase transition of order $2\frac{1}{2}$: appearance of a new cavity (a); breaking of neck accompanied either by the appearance of a line of O -points (b) or the disappearance of X -points (c) (the lines of parabolic points are shown dashed).

the surface $\varepsilon(\mathbf{p}) = \varepsilon_k$ contains a point at which the velocity becomes zero [$\mathbf{v}(\mathbf{p}_k) = 0$]. Usually (at $P = 0$), the Fermi energy is $\varepsilon_F \neq \varepsilon_k$ and the presence of the van Hove singularities manifests itself only indirectly (for example, through the complexity of the Fermi surface of a number of metals; see above and the next Section). The application of pressure will "drive" the van Hove singularity off the Fermi level. As a result, the Fermi surface will change its connectivity at $P = P_k$. This is reflected in the fact that the density of electronic states is of the form $\nu(\varepsilon_F) \sim \sqrt{P - P_k}$, so that, when $T = 0$, this can be interpreted in the Ehrenfest nomenclature as a phase transition of order $2\frac{1}{2}$.⁴¹ It is clear from the foregoing that, when $P = P_k$, the Fermi surface contains a point (or points) at which $\nu = 0$.

The presence of slow electrons with $\nu = 0$ on the critical Fermi surface (for $P = P_k$) leads to anomalies in both thermodynamic and transport properties. The formulas listed in Table III show that the properties of a metal that are due to interaction between electrons and the sound wave are particularly sensitive to a change in the connectivity of the Fermi surface. Although the change in the Fermi surface occurs at individual points in \mathbf{p} -space, the macroscopic sound absorption coefficient exhibits a finite jump when a new cavity is formed, or even a logarithmically diverging singularity (at $T = 0$ and $kl = \infty$) when a neck is broken.⁸⁵

A change in the connectivity of the Fermi surface (breaking or formation of a neck) is accompanied by a change in the local geometry of the surface: breaking of the neck is accompanied either by the appearance of a line of O -points, or the disappearance of a line of X -points (Fig. 32). This means that, in the case of phase transitions of order $2\frac{1}{2}$ that are due to the breaking of a neck, one should observe the appearance (or disappearance) of anomalies in the dependence of Γ_e on the direction of propagation of sound (see Fig. 30). It is shown in⁸⁶ that, in this case, these anomalies are particularly sharp because of the proximity of the line of parabolic points to the conical point in \mathbf{p} -space (at which $\nu = 0$!).

A change in the connectivity of the Fermi surface is not essential for the appearance or disappearance of a line of parabolic points. It is sufficient to produce a crater on the Fermi surface (Fig. 33). Depending on

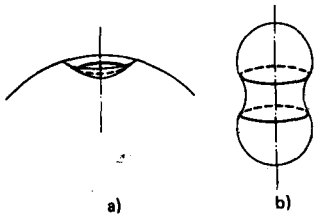


FIG. 33. Formation of a crater (a) and neck (b) on a Fermi surface is accompanied by the appearance of lines of parabolic points (thick lines). The belt corresponding to the direction of propagation of sound perpendicular to the axis of the Fermi surface runs around the crater.

the nature of the point at which the Fermi surface becomes flat, one obtains either a crater (Fig. 33a) or a waist (Fig. 33b). These "events" are necessarily accompanied by the appearance or disappearance of angular singularities in Γ ,⁸⁶ and many other anomalies (change in the spectrum of Pippard frequencies in a magnetic field,⁸⁰ change in the spectrum of de Haas-van Alphen oscillations,⁸⁷ and so on).

The last paragraph enables us to generalize the idea of a topologic transition (as of the phase transition of order $2\frac{1}{2}$ is sometimes called) to any change in the geometry of the Fermi surface that is accompanied by a qualitative change in some characteristics of the metal.

In conclusion, one final prediction⁸⁸: according to (22), the absorption coefficient $\Gamma^{\text{phon}}(\mathbf{H})$ in a relatively strong magnetic field will increase with increasing electron mean free time τ . As already noted, a rough estimate of the mean free path l shows that l is weakly dependent on the number of electrons. This means that the relaxation time $\tau = l/v_F$ should increase with decreasing size of the cavity in the Fermi surface (prior to its disappearance at $P = P_A$; see Fig. 32), leading to an increase in $\Gamma^{\text{phon}}(\mathbf{H})$. Of course, this growth ceases in the immediate neighborhood of the phase transition of order $2\frac{1}{2}$ and $\Gamma^{\text{phon}}(\mathbf{H})$ vanishes: an electron whose velocity is less than the velocity of sound cannot absorb a phonon.

11. TRANSFER OF ELECTRONS FROM ONE ORBIT TO ANOTHER. MAGNETIC BREAKTHROUGH

In all the phenomena described above, the electrons were either at a definite point in \mathbf{p} -space on the Fermi surface or they hopped over from one point to another as a result of scattering or, finally, they moved over classical trajectories in the magnetic field. The recognition of the complexity of the Fermi surface of most metals is connected in particular with the understanding of the fact that classical electron trajectories in a magnetic field (in \mathbf{p} -space) have points of closest approach, so that we have the possibility of a tunnel transition from one trajectory to another. This phenomenon has been referred to as magnetic breakthrough⁸⁹ and has been found to play a fundamental role in many properties of metals.⁹⁰

To understand the nature and importance of magnetic breakthrough, we must distinguish between intra- and interband transitions. If we confine our attention to the

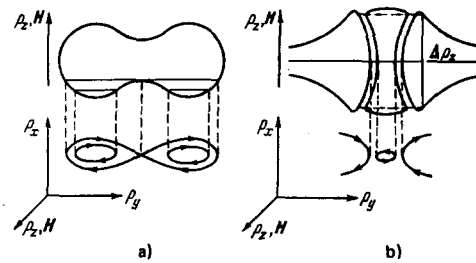


FIG. 34. Intraband breakthrough involves participation of electrons from a thin layer near a self-intersecting path (a), whereas interband breakthrough involves electrons from a layer of finite thickness Δp_x (b). In both cases, we show the paths in \mathbf{p} -space.

Fermi surface, intraband transitions are possible in narrow intervals of values of p_x (Fig. 34a), whereas interband transitions are possible within broad bands of width of the order of \hbar/a (Fig. 34b). Magnetic breakthrough is defined as the range of phenomena connected with interband transitions.

We shall not go into details of the properties of metals under the conditions of magnetic breakthrough and will merely note some of the points that enable us to achieve simple geometrical interpretations.

The region of magnetic breakthrough is the region in which classical paths approach one another. This means that an electronic state in the magnetic breakthrough configuration is a superposition of quasiclassical states. This is why one can use geometric ideas in the study of magnetic breakthrough, whereas physical quantities characterizing a metal in the course of magnetic breakthrough can be expressed in the language of the dispersion relation and unitary \hat{s} -matrices of rank two, which describe the two-channel scattering in the magnetic breakthrough regions.¹¹⁾ The fact that the magnetic breakthrough region is small in comparison with the size of classical regions of magnetic breakthrough configurations enables us to evaluate the \hat{s} -matrix for an arbitrary magnetic field without violating the quasiclassical condition imposed on motion between breakthrough regions⁹² ($\hbar\omega_c \ll \epsilon_F$). When the breakthrough probability W is not zero or unit ($0 < W < 1$), the

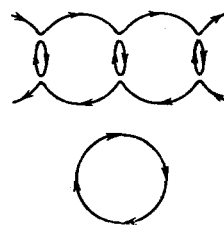


FIG. 35. Magnetic breakthrough can change the topology of electron paths. In a low field in the absence of breakthrough, there are both open and closed paths; in a high field, only the closed path is possible (lower part of figure).

¹¹⁾ The square of the modulus of the off-diagonal element of the \hat{s} -matrix is the probability W of breakthrough, and the square of the modulus of the diagonal element is the probability $1 - W$ that breakthrough will not take place.⁹¹

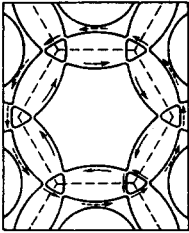


FIG. 36. Magnetic breakthrough trajectories found from studies of the de Haas-van Alphen effect in magnesium.

motion of electrons is quantum-mechanical in character, but $W \rightarrow 1$ as the magnetic field increases and the motion again becomes quasiclassical. However, electrons then acquire certain new features which they did not have in weak fields. In view of the spectroscopic character of studies performed in strong magnetic fields, we must introduce a work of caution; the changes can be not merely qualitative but even quantitative. Figure 35 shows that magnetic breakthrough may lead to a change in the topology of a plane cross section, transforming it from an open to a closed configuration.

The phenomena due to magnetic breakthrough were first discovered experimentally by Priestley,⁹³ who examined the de Haas-van Alphen effect in magnesium and found periods (closed cross sections) due to electron tunneling through barriers separating classical paths (Fig. 36).

Magnetic breakthrough can be the source of many unusual oscillation effects that cannot be reduced to de Haas-van Alphen oscillations. There are cases where two or even three large orbits on the Fermi surface connect with one another because of magnetic breakthrough across a small orbit (Fig. 37). It is possible to introduce the idea of the effective breakthrough probability W_{eff} that an electron will undergo transition from one large quasiclassical region to another. This effective probability is a periodic function of the reciprocal magnetic field. The period is given by the same formula that is used for the de Haas-van Alphen effect, i.e., (9). However, the origin of the periodic dependence is different. It is now due to interference between waves reflected from the breakthrough points. The periodicity arises for the same reason as in the case of the coefficient of transparency of a dielectric plate in which electromagnetic waves interfere with one another. Oscillations in $W_{\text{eff}} = W_{\text{eff}}(H)$ are the reason for the giant oscillations in galvanomagnetic characteristics that involve the main groups of electrons in a metal (Fig. 38). This can be referred to as the relay effect. The small

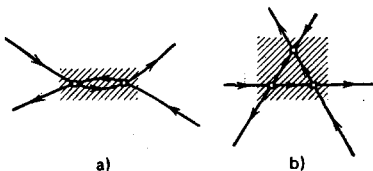


FIG. 37. Small orbits couple larger ones as a result of magnetic breakthrough. The shaded regions may act as the effective regions of magnetic breakthrough.

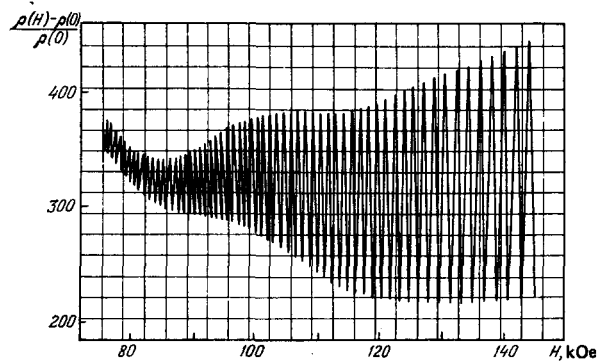


FIG. 38. Giant oscillations in the magnetoresistance of beryllium due to magnetic breakthrough. The measurements were carried out by the International Laboratory for Strong Fields and Low Temperatures. Wrockaw, Poland, in 1972.

region acts as a relay that controls the motion of electrons on a large trajectory because of magnetic breakthrough.⁹⁴

Interference between electron waves arriving at a given point of the magnetic-breakthrough configuration can also be the reason for oscillation effects. For this to happen, two paths must be very similar to one another, as shown in Fig. 39. The oscillation period is, as before, determined by "area" quantization. The word area is given in quotes in order to emphasize that there are no electrons that describe this area. This type of interference is observed only in transport phenomena,⁹⁵ whereas the oscillating part of thermodynamic characteristics is determined by closed loops.

Magnetic breakthrough has been discovered in many metals and properties. Its manifestations are very varied and an understanding of magnetic breakthrough phenomena is important for the interpretation of the energy spectra of metals because, during the breakthrough process, electrons are found in regions of p-space that are inaccessible to classical motion.

12. CONCLUDING REMARKS

Our constructions are unrelated to modern geometry. Physicists interested in the theory of metals would not claim to have discovered anything new in geometry. Geometry is merely used in the electronic theory of metals in order to visualize many conclusions and results. Physicists are attracted by the fact that many of the properties of metals are due to electrons occupying a surface, the cross section and certain lines and points of which have a clear physical meaning. Our understanding of the nature of metals has now reached a state where we know how to construct these surfaces,



FIG. 39. Electrons moving on neighboring paths interfere and this leads to oscillations in transport characteristics. The period in the magnetic field is determined by the shaded region. Points represent the region of magnetic breakthrough.

how to draw the lines on them, and how to determine the position of the required points. We also know how the simple geometric ideas can be used to calculate different physical parameters.

We should like to take this opportunity to thank L. P. Pitaevskii for useful suggestions, and T. Yu. Lisovskaya and Sh. T. Mevlyut for assistance in the preparation of this review for publication.

- ¹I. M. Lifshitz, Zh. Eksp. Teor. Fiz. **26**, 551 (1954) [Sov. Phys. JETP **26**, 551 (1954)].
- ²L. D. Landau, *Sobranie trudov* (Collected Papers), Vol. 2, Nauka, M., 1969, p. 328.
- ³L. D. Landau and J. M. Luttinger, quoted in: A. A. Abrikosov, L. P. Gor'kov, and I. E. Dzyaloshinskii, *Metody kvantovoi teorii polya v statisticheskoi fizike* (Methods of Quantum Field Theory in Statistical Physics) Fizmatgiz, M., 1962 (English. Transl. published by Prentice-Hall, 1963).
- ⁴I. M. Lifshits, M. Ya. Azbel', and M. I. Kaganov, *Elektronnaya teoriya metallov* (Electron Theory of Metals), Nauka, M., 1971.
- ⁵H. London, Proc. R. Soc. London Ser. A **176**, 522 (1940). A. B. Pippard, *ibid.* **191**, 385 (1947). G. E. Reuter and E. H. Sondheimer, *ibid.* **195**, 336 (1948). I. M. Lifshits and M. I. Kaganov, Usp. Fiz. Nauk **69**, 49 (1959) [Sov. Phys. Usp. **2**, 831 (1960)].
- ⁷D. Shoenberg, Proc. R. Soc. London Ser. A **170**, 341 (1939); the appendix to this paper gives the theory of the de Haas-van Alphen effect [see also L. D. Landau, *Sobr. trudov* (Collected Papers), Vol. 1, Nauka, M., 1969].
- ⁸H. Jones, Proc. R. Soc. London Ser. A **155**, 653 (1936).
- ⁹I. M. Lifshits and A. M. Kosevich, Dokl. Akad. Nauk SSSR **96**, 963 (1954); Zh. Eksp. Teor. Fiz. **29**, 730 (1955) [Sov. Phys. JETP **2**, 636 (1956)].
- ¹⁰I. M. Lifshits, Doklad na sessii AN USSR, Kiev (Paper read at a meeting of the Academy of Sciences of the Ukrainian SSR, Kiev).
- ¹¹L. Onsager, Philos. Mag. **43**, 1006 (1952).
- ¹²I. M. Lifshits and A. V. Pogorelov, Dokl. Akad. Nauk SSSR **96**, 1143 (1954).
- ¹³E. M. Gunnarsen, Philos. Trans. R. Soc. London Ser. A **249**, 299 (1956); A. V. Gold, *ibid.* **251**, 85 (1958).
- ¹⁴E. Sondheimer, Phys. Rev. **80**, 401 (1950).
- ¹⁵A. B. Pippard, Philos. Mag. **2**, 1147 (1957).
- ¹⁶E. A. Kaner and V. F. Gantmakher, Usp. Fiz. Nauk **94**, 123 (1968) [Sov. Phys. Usp. **11**, 81 (1968)].
- ¹⁷I. M. Lifshits and A. M. Kosevich, Dokl. Akad. Nauk SSSR **91**, 795 (1953).
- ¹⁸Yu. P. Gaidukov and E. M. Golyamina, Pis'ma Zh. Eksp. Teor. Fiz. **29**, 336 (1976) [JETP Lett. **23**, 301 (1976)].
- ¹⁹I. M. Lifshits, M. Ya. Azbel' and M. I. Kaganov, Zh. Eksp. Teor. Fiz. **31**, 63 (1956) [Sov. Phys. JETP **4**, 41 (1957)].
- ²⁰I. M. Lifshits and V. G. Peschanskiĭ, Zh. Eksp. Teor. Fiz. **35**, 1251 (1958) [Sov. Phys. JETP **8**, 875 (1959)].
- ²¹N. E. Alekseevskii, Yu. P. Gaidukov, I. M. Lifshits, and V. G. Peschanskiĭ, Zh. Eksp. Teor. Fiz. **39**, 1201 (1960) [Sov. Phys. JETP **12**, 837 (1961)].
- ²²M. Ya. Azbel', Zh. Eksp. Teor. Fiz. **44**, 983 (1963) [Sov. Phys. JETP **17**, 667 (1963)].
- ²³M. Ya. Azbel' and V. G. Peschanskiĭ, Zh. Eksp. Teor. Fiz. **49**, 572 (1965) [Sov. Phys. JETP **22**, 399 (1966)]; **55**, 1980 (1968) [**29**, 1045 (1969)].
- ²⁴R. G. Mints, Pis'ma Zh. Eksp. Teor. Fiz. **9**, 629 (1969) [JETP Lett. **9**, 387 (1969)].
- ²⁵A. V. Shubnikova and V. de Haas, Comm. Kamerling Onnes Lab. Univ. Leiden **19**, 207a (1930); V. G. Lazarev, N. M. Makhimovich, and E. A. Pargenova, Zh. Eksp. Teor. Fiz. **9**, 1169 (1939).
- ²⁶S. Titeica, Ann. Phys. (Utrecht) **22**, 128 (1935); A. I. Akhiezer, Zh. Eksp. Teor. Fiz. **9**, 426 (1939); B. I. Davydov and I. Ya. Pomeranchuk, *ibid.* p. 1294; G. E. Zil'berman, Zh. Eksp. Teor. Fiz. **29**, 762 (1955) [Sov. Phys. JETP **2**, 650 (1957)]; I. M. Lifshits, Zh. Eksp. Teor. Fiz. **32**, 1509 (1957) [Sov. Phys. JETP **5**, 1227 (1957)]; I. M. Lifshits and A. M. Kosevich, Zh. Eksp. Teor. Fiz. **38**, 188 (1960) [Sov. Phys. JETP **11**, 137 (1960)]; E. N. Adams and T. D. Holstein, J. Phys. Chem. Solids **10**, 254 (1959); A. M. Kosevich and V. V. Andreev, Zh. Eksp. Teor. Fiz. **38**, 882 (1960) [Sov. Phys. JETP **11**, 637 (1960)].
- ²⁷N. E. Alekseevskii, N. B. Brandt, and T. I. Kostina, Dokl. Akad. Nauk SSSR **105**, 46 (1955).
- ²⁸M. I. Kaganov and V. G. Peschanskiĭ, Zh. Eksp. Teor. Fiz. **35**, 1052 (1958) [Sov. Phys. JETP **8**, 734 (1959)].
- ²⁹M. I. Kaganov, A. M. Kadigrobov, and A. A. Slutskii, Zh. Eksp. Teor. Fiz. **53**, 1135 (1967) [Sov. Phys. JETP **26**, 670 (1968)].
- ³⁰I. M. Lifshits, Zh. Eksp. Teor. Fiz. **18**, 1135 (1948).
- ³¹V. B. Fiks, Fiz. Tverd. Tela (Leningrad) **5**, 2213 (1963) [Sov. Phys. Solid State **5**, 1611 (1964)]; M. I. Kaganov, I. M. Lifshits, and V. B. Fiks, Fiz. Tverd. Tela (Leningrad) **6**, 2723 (1964) [Sov. Phys. Solid State **6**, 2167 (1965)].
- ³²R. E. Peierls, Quantum Theory of Solids, Oxford University Press, 1964 (Russ. Transl. IL, M., 1956).
- ³³A. B. Pippard, Proc. R. Soc. London Ser. A **308**, 291 (1968).
- ³⁴R. A. Joung, Phys. Rev. **175**, 813 (1968).
- ³⁵R. N. Gurzhi and A. I. Kopeliovich, Zh. Eksp. Teor. Fiz. **71**, 635 (1976) [Sov. Phys. JETP **44**, 334 (1976)].
- ³⁶E. I. Rashba, Z. S. Gribnikov, and V. Ya. Kravchenko, Usp. Fiz. Nauk **119**, 3 (1976) [Sov. Phys. Usp. **19**, 361 (1976)].
- ³⁷W. A. Harrison, Pseudopotentials in the Theory of Metals, Benjamin, N. Y., 1966 (Russ. Transl., Mir, M., 1968).
- ³⁸L. Brillouin, Wave Propagation in Periodic Structures, N. Y., 1976.
- ³⁹V. Heine, M. L. Cohen, and D. Weaire, Pseudopotential Theory, in: Solid State Physics: Advances in Research and Applications, Academic Press, London, 1970 [Russian transl., Mir, M., (1968)].
- ⁴⁰I. E. Dzyaloshinskii, Zh. Eksp. Teor. Fiz. **47**, 336 (1964) [Sov. Phys. JETP **20**, 223 (1965)].
- ⁴¹I. M. Lifshits, Zh. Eksp. Teor. Fiz. **30**, 1509 (1956) [Sov. Phys. JETP **5**, 1227 (1957)].
- ⁴²L. Van Hove, Phys. Rev. **89**, 1189 (1953).
- ⁴³L. D. Landau, *Sbor. trudov* (Collected Papers), Vol. 2, Nauka, M., 1969, p. 7.
- ⁴⁴A. B. Pippard, Proc. R. Soc. London Ser. A **91**, 385 (1947); **224**, 273 (1954).
- ⁴⁵A. B. Pippard, Philos. Mag. **46**, 1104 (1955).
- ⁴⁶A. I. Akhiezer, M. I. Kaganov, and G. Ya. Lyubarskiĭ, Zh. Eksp. Teor. Fiz. **32**, 837 (1957) [Sov. Phys. JETP **5**, 685 (1957)].
- ⁴⁷M. I. Kaganov and M. Ya. Azbel', Dokl. Akad. Nauk SSSR **102**, 49 (1955).
- ⁴⁸A. B. Pippard, Trans. R. Soc. Ser. A **250**, 325 (1957).
- ⁴⁹A. I. Akhiezer, Zh. Eksp. Teor. Fiz. **8**, 1330 (1938).
- ⁵⁰H. Frölich, Phys. Rev. **79**, 845 (1950).
- ⁵¹J. A. Rayne and C. K. Jones, "Ultrasonic attenuation in normal metals and superconductors: Fermi-surface effects," in: Physical Acoustics, Vol. 7, Academic Press, N. Y., 1970.
- ⁵²M. Ya. Azbel' and E. A. Kaner, Zh. Eksp. Teor. Fiz. **30**, 811 (1956) [Sov. Phys. JETP **3**, 772 (1956)]; **32**, 896 (1957) [**5**, 730 (1957)]; Phys. Chem. Solids **6**, 113 (1958).
- ⁵³E. Fawcett, Phys. Rev. **103**, 1582 (1956).
- ⁵⁴M. S. Khaikin, Zh. Eksp. Teor. Fiz. **42**, 27 (1962) [Sov. Phys. JETP **15**, 18 (1962)].
- ⁵⁵E. A. Kaner and V. G. Skobov, Usp. Fiz. Nauk **89**, 367 (1966) [Sov. Phys. Usp. **9**, 480 (1967)]; Adv. Phys. **17**, 69 (1968).

- ⁵⁶O. V. Konstantinov and V. I. Perel, *Zh. Eksp. Teor. Fiz.* **38**, 161 (1960) [*Sov. Phys. JETP* **11**, 117 (1960)]; P. Agrain, in: *Proc. Intern. Conf. on Semiconductor Physics, Prague, 1964*, p. 224.
- ⁵⁷S. J. Buchsbaum and T. K. Galt, *Phys. Fluids* **4**, 1514 (1961). E. A. Kaner and V. G. Skobov, *Zh. Eksp. Teor. Fiz.* **45**, 610 (1963) [*Sov. Phys. JETP* **18**, 419 (1964)]; M. S. Khaikin, L. A. Fal'kovskii, V. S. Édel'man, and R. T. Mina, *ibid.*, p. 1704 [*Sov. Phys. JETP* **18**, 1167 (1964)].
- ⁵⁸A. W. Overhauser and S. Rodriguez, *Phys. Rev.* **141**, 429 (1966); J. C. McGroddy, J. R. Stanford, and E. A. Stern, *Phys. Rev.* **141**, 437 (1966). L. M. Fisher, V. V. Lavrova, V. A. Yudin, O. V. Konstantinov, and V. G. Skobov, *Zh. Eksp. Teor. Fiz.* **60**, 759 (1971) [*Sov. Phys. JETP* **33**, 410 (1971)]; V. G. Skobov, Appendix to the book by P. M. Platzman and P. A. Wolff, *Waves and Interactions in Solid-State Plasmas*, Academic Press, New York, 1972.
- ⁵⁹V. Ya. Demikhovskii and S. S. Savinskiĭ, *Fiz. Tverd. Tela (Leningrad)* **18**, 2262 (1976) [*Sov. Phys. Solid State* **18**, 1318 (1976)].
- ⁶⁰V. M. Agranovich and V. L. Ginzburg, *Élektrodinamika sred s prostranstvennoĭ dispersiei* (Electrodynamics of Media With Spatial Dispersion), Nauka, M., 1979.
- ⁶¹V. Ya. Demikhovskii and A. P. Protagenov, *Usp. Fiz. Nauk* **118**, 101 (1976) [*Sov. Phys. Usp.* **19**, 53 (1976)].
- ⁶²V. L. Gurevich, *Zh. Eksp. Teor. Fiz.* **37**, 71 (1959) [*Sov. Phys. JETP* **10**, 51 (1960)].
- ⁶³É. A. Kaner, V. G. Peschanskiĭ, and I. A. Privorotskiĭ, *Zh. Eksp. Teor. Fiz.* **40**, 214 (1961) [*Sov. Phys. JETP* **13**, 147 (1961)]; K. Fuchs, *Proc. Camb. Philos. Soc.* **34**, 100 (1938).
- ⁶⁴M. Ya. Azbel' and M. I. Kaganov, *Zh. Eksp. Teor. Fiz.* **27**, 762 (1954).
- ⁶⁵B. N. Aleksandrov and M. I. Kaganov, *Zh. Eksp. Teor. Fiz.* **41**, 1333 (1961) [*Sov. Phys. JETP* **14**, 948 (1962)].
- ⁶⁶See, for example: A. F. Andreev, *Usp. Fiz. Nauk* **105**, 113 (1971) [*Sov. Phys. Usp.* **14**, 609 (1971)].
- ⁶⁷S. S. Nedozerov, *Zh. Eksp. Teor. Fiz.* **51**, 868 (1966) [*Sov. Phys. JETP* **24**, 578 (1967)].
- ⁶⁸Yu. F. Ogrin, V. N. Lutskiĭ, and M. I. Elinson, *Pis'ma Zh. Eksp. Teor. Fiz.* **3**, 114 (1966) [*JETP Lett.* **3**, 71 (1966)]; V. N. Lutskiĭ, D. N. Korneev, and M. I. Elinson, *ibid.* **4**, 267 (1966) [*JETP Lett.* **4**, 179 (1966)].
- ⁶⁹M. S. Khaikin, *Zh. Eksp. Teor. Fiz.* **39**, 212 (1960) [*Sov. Phys. JETP* **12**, 152 (1961)]; **55**, 1696 (1968) [**28**, 829 (1969)]; *Usp. Fiz. Nauk* **96**, 409 (1968) [*Sov. Phys. Usp.* **11**, 785 (1968)].
- ⁷⁰T. W. Nee and R. E. Prange, *Phys. Lett. A* **25**, 582 (1967).
- ⁷¹M. A. Lur'e and V. G. Peschanskiĭ, *Vkn. XVII Vsesoyuznoe soveshchanie po fizike nizkikh temperatur (in: Proc. Seventeenth All-Union Conf. on Low-Temperature Physics)*, Donetsk, 1972. O. V. Kirichenko, M. A. Lur'e, and V. G. Peschanskiĭ, *Zh. Eksp. Teor. Fiz.* **70**, 337 (1975) [*Sov. Phys. JETP* **43**, 175 (1976)].
- ⁷²A. P. Volodin, M. S. Khaikin, and V. S. Édel'man, *Pis'ma Zh. Eksp. Teor. Fiz.* **17**, 491 (1973) [*JETP Lett.* **17**, 353 (1973)]; *Zh. Eksp. Teor. Fiz.* **65**, 2105 (1973) [*Sov. Phys. JETP* **38**, 1052 (1974)].
- ⁷³M. S. Khaikin and V. S. Édel'man, *Zh. Eksp. Teor. Fiz.* **47**, 878 (1964) [*Sov. Phys. JETP* **20**, 587 (1964)]; V. G. Peschanskiĭ, *Pis'ma Zh. Eksp. Teor. Fiz.* **7**, 489 (1968) [*JETP Lett.* **7**, 375 (1968)]; O. V. Kirichenko, M. A. Lur'e, and V. G. Peschanskiĭ, *Fiz. Nizk. Temp.* **2**, 858 (1976) [*Sov. J. Low Temp. Phys.* **2**, 421 (1976)].
- ⁷⁴A. B. Migdal, *Zh. Eksp. Teor. Fiz.* **34**, 1438 (1958) [*Sov. Phys. JETP* **7**, 996 (1958)]; W. Kohn, *Phys. Rev. Lett.* **2**, 393 (1959).
- ⁷⁵M. I. Kaganov and A. I. Semenenko, *Zh. Eksp. Teor. Fiz.* **50**, 630 (1966) [*Sov. Phys. JETP* **23**, 419 (1966)].
- ⁷⁶A. M. Afanas'ev and Yu. Kagan, *Zh. Eksp. Teor. Fiz.* **43**, 1456 (1962) [*Sov. Phys. JETP* **16**, 1030 (1963)].
- ⁷⁷D. Shoenberg and I. M. Templeton, *Physica (Utrecht)* **69**, 293 (1973).
- ⁷⁸M. Ya. Azbel', *Zh. Eksp. Teor. Fiz.* **39**, 1276 (1960) [*Sov. Phys. JETP* **12**, 891 (1961)].
- ⁷⁹G. T. Avanesyan, M. I. Kaganov, and T. Yu. Lisovskaya, *Pis'ma Zh. Eksp. Teor. Fiz.* **25**, 381 (1977) [*JETP Lett.* **25**, 355 (1977)]; *Zh. Eksp. Teor. Fiz.* **75**, 1736 (1978) [*Sov. Phys. JETP* **48**, 900 (1978)].
- ⁸⁰V. M. Kontorovich and N. A. Stepanova, *Pis'ma Zh. Eksp. Teor. Fiz.* **18**, 381 (1973) [*JETP Lett.* **18**, 223 (1973)].
- ⁸¹V. M. Kontorovich and N. A. Stepanova, *Fiz. Tverd. Tela (Leningrad)* **20**, 245 (1978) [*Sov. Phys. Solid State* **20**, 137 (1978)]; *Zh. Eksp. Teor. Fiz.* **76**, 642 (1979) [*Sov. Phys. JETP* **49**, 321 (1979)].
- ⁸²M. I. Kaganov and T. Yu. Lisovskaya, *Lectures Given at the Winter School on Theoretical Physics, Karpach, Poland, 1979*.
- ⁸³J. M. Ziman, *Principles of Solid-State Theory*, Cambridge Univ. Press, 1964 (Russ. transl., Mir, M., 1974).
- ⁸⁴N. V. Zavaritskiĭ, M. I. Kaganov, and Sh. T. Mevlyut, *Pis'ma Zh. Eksp. Teor. Fiz.* **28**, 223 (1978) [*JETP Lett.* **28**, 205 (1978)].
- ⁸⁵V. N. Davydov and M. I. Kaganov, *Pis'ma Zh. Eksp. Teor. Fiz.* **16**, 133 (1972) [*JETP Lett.* **16**, 92 (1972)].
- ⁸⁶M. I. Kaganov and T. L. Lobanova, *Zh. Eksp. Teor. Fiz.* **77**, 1590 (1979) [*Sov. Phys. JETP* **50**, 797 (1979)].
- ⁸⁷N. B. Brandt, V. V. Moshchalkov, and S. M. Chudinov, *Pis'ma Zh. Eksp. Teor. Fiz.* **25**, 361 (1977) [*JETP Lett.* **25**, 336 (1977)]; *Zh. Eksp. Teor. Fiz.* **74**, 1829 (1978) [*Sov. Phys. JETP* **47**, 953 (1978)].
- ⁸⁸T. V. Ivanov and M. I. Kaganov, *Fiz. Nizk. Temp.* **5**, 158 (1979) [*Sov. J. Low Temp. Phys.* **5**, 75 (1979)].
- ⁸⁹M. H. Cohen and Z. M. Falicov, *Phys. Rev. Lett.* **7**, 231 (1961).
- ⁹⁰R. W. Stark and L. M. Falicov, in: *Progress in Low Temperature Physics, Vol. 5*, North-Holland, Amsterdam, 1967, p. 235.
- ⁹¹A. A. Slutskii, *Zh. Eksp. Teor. Fiz.* **58**, 1098 (1970) [*Sov. Phys. JETP* **31**, 589 (1970)].
- ⁹²E. T. Blount, *Phys. Rev.* **126**, 1636 (1962).
- ⁹³M. G. Priestley, *Proc. R. Soc. London Ser. A* **276**, 258 (1963).
- ⁹⁴L. M. Falicov, A. B. Pippard, and P. R. Sievert, *Phys. Rev.* **151**, 498 (1966). N. E. Alekseevskii, A. A. Slutskii, and V. S. Egorov, *J. Low Temp. Phys.* **5**, 377 (1971).
- ⁹⁵R. W. Stark and C. B. Friedberg, *Phys. Rev. Lett.* **26**, 556 (1971); *Phys. Rev. B* **5**, 2844 (1972); see also Ref. 91.

Translated by S. Chomet
 Edited by Morton Hamermesh